

Radiative CP violation in the Higgs sector of the Next-to-minimal supersymmetric model

S.W. Ham⁽¹⁾, Y.S. Jeong⁽²⁾, S.K. Oh^(1;2)

⁽¹⁾ Center for High Energy Physics, Kyungpook National University
Daegu 702-701, Korea

⁽²⁾ Department of Physics, Konkuk University, Seoul 143-701, Korea

Abstract

We investigate the neutral Higgs sector in the next-to-minimal supersymmetric standard model (NMSSM) with explicit CP violation at the one-loop level by using the effective potential method. In general, explicit CP violation is possible at the tree-level in the Higgs potential of the NMSSM, which may possess a complex phase. The tree-level Higgs potential can be made CP conserving by assuming that all the relevant parameters are real. However, we find that the CP-conserving Higgs potential at the tree-level may still develop complex phases at the one-loop level through radiative corrections. These complex phases exhibit explicit CP violation in the mixings between the scalar and pseudoscalar Higgs bosons. It is observed that the complex phase from the neutralino sector contributes relatively dominantly to scalar-pseudoscalar mixings. Meanwhile the neutral Higgs boson masses are roughly stable against the variation of that complex phase.

I. Introduction

Supersymmetry (SU SY) must be broken in order to be realized in the nature. In various supersymmetric models, the SU SY breaking may be accomplished by introducing soft SU SY breaking terms. The introduction of soft SU SY breaking terms may also invoke irreducible complex phases. These complex phases may contribute to the mixing between the scalar and pseudoscalar Higgs bosons, thus account for explicit CP violation. In the minimal supersymmetric standard model (MSSM), there can be as many as eleven non-trivial phases associated with the scalar fermions, the charginos, and the neutralinos. However, at the tree level, the MSSM can avoid explicit CP violation by adjusting the complex phases away via redefinition of various participating fields in the model. It has been found that, at the one-loop level the MSSM can accommodate explicit CP violation in its neutral Higgs sector [1]. Many authors have investigated the explicit CP violation in the MSSM in the radiatively corrected Higgs potential [1-4], where a few complex phases (three from the scalar fermion sector of the third generation, one from the charginos, and one from the neutralinos) can participate in the scalar-pseudoscalar mixing.

Unlike in the case of the MSSM, explicit CP violation can be realized in the next-to-minimal supersymmetric standard model (NMSSM) even at the tree level. At the tree level in the Higgs potential of the NMSSM, a nontrivial complex phase emerges after redefining the three Higgs fields [5]. This complex phase from the tree-level Higgs potential may persist in the one-loop effective potential if the scalar top quarks are degenerate in mass. In Ref.[5], assuming the degeneracy of the scalar top quark masses, the scalar pseudoscalar mixing is investigated in the NMSSM with explicit CP violation. It has been shown that large mixings between the scalar and pseudoscalar Higgs bosons may be realized as the vacuum expectation value (VEV) of the neutral Higgs singlet approaches to the electroweak scale [5].

We have elsewhere investigated the implications of the mass splitting between the scalar quarks of the third generation in the NMSSM at the one-loop level with explicit CP violation [6]. In this case, two additional complex phases are induced from the scalar top and scalar bottom quark masses. We have then extended our investigations to the chargino sector in the NMSSM with explicit CP violation [7]. An additional complex phase other than the tree-level phase appearing from the mixing between the chargino masses is shown to contribute the scalar-pseudoscalar mixing, too, at the one-loop level.

In this paper, we investigate the possibility where the tree-level Higgs potential is CP conserving while explicit CP violation occurs in the Higgs sector of the NMSSM through the one-loop radiative corrections. We assume that the tree-level complex phase is zero. All the parameters in the NMSSM Higgs potential at the tree level are assumed to be real. Then, the possible sources of complex phases contributing to the scalar-pseudoscalar mixing are the radiative corrections from the scalar top, the scalar bottom, the scalar tau lepton, the chargino, and the neutralino sectors. In fact, in the one-loop effective potential for each sector may be embedded a complex phase. We investigate the effects of these a few complex phases in the radiatively corrected Higgs potential of the NMSSM. We find that the complex phase from the neutralino sector gives relatively large changes to the scalar-pseudoscalar mixing.

Our paper is organized as follows. In Sec. II we briefly describe the Higgs sector of the NMSSM at the tree level. In Sec. III, for the scenario of explicit CP violation, radiative corrections from the scalar top quark sector, the scalar bottom quark sector, the scalar tau lepton sector, the chargino sector, and the neutralino sector are explicitly calculated using the effective potential method. Numerical analyses and results for the explicit CP violation at the one-loop level are presented in Sec. IV. Conclusions and some remarks are given in Sec.

V. Appendices supply the formulae for the elements of the mass matrix of the neutral Higgs bosons, which contain the radiative corrections from each sector of the scalar top quarks, the scalar bottom quarks, the scalar tau leptons, the charginos, and the neutralinos.

II. The Higgs sector

The NMSSM has two SU(2) doublet superfields $H_1 = (H_1^0; H_1^-)$ and $H_2 = (H_2^+; H_2^0)$ with hypercharges $Y=1/2$ and $Y=1/2$, respectively, and a neutral SU(2) singlet superfield N with zero-hypercharge. For the fermion matter fields, we take into account only the third generation of quarks and leptons. The general form of the NMSSM superpotential may be expressed as

$$W = h_t Q H_2 t_R^c + h_b Q H_1 b_R^c + h_L L H_1 e_R^c + \lambda N H_1 H_2 + \frac{k}{3} N^3; \quad (1)$$

where $H_1 H_2 = H_1^0 H_2^0 - H_1^- H_2^+$, and all the coupling coefficients are dimensionless. The chiral superfields Q and L contain the left-handed quark and lepton doublets, and t_R^c, b_R^c and e_R^c are the charge conjugate of the right-handed t quark, b quark, and lepton, respectively, and the parameters h_t, h_b , and h_L are their respective Yukawa coupling coefficients.

In the NMSSM [8, 9], the tree-level Higgs potential may be decomposed into three parts as

$$V^0 = V_D + V_F + V_S;$$

where

$$\begin{aligned} V_D &= \frac{g_1^2}{8} (H_1^y \sim H_1 + H_2^y \sim H_2)^2 + \frac{g_2^2}{8} (\mathbb{H}_2^j - \mathbb{H}_1^j)^2; \\ V_F &= \lambda^2 [(\mathbb{H}_1^j + \mathbb{H}_2^j) N^j + \mathbb{H}_1 H_2^j] + k^2 N^4 \quad (\lambda, k, A, \text{ and } A_k \text{ are real}); \\ V_S &= m_{H_1}^2 \mathbb{H}_1^j + m_{H_2}^2 \mathbb{H}_2^j + m_N^2 N^j \quad (A, m_{H_1}, m_{H_2}, \text{ and } m_N \text{ are real}); \end{aligned} \quad (2)$$

with g_1 and g_2 being the U(1) and SU(2) gauge coupling constants, respectively, and $\sim = (\tau^1, \tau^2, \tau^3)$ are the Pauli matrices. The soft SUSY breaking V_S has two additional parameters A and A_k , both of mass dimension, and three soft masses m_{H_1}, m_{H_2} , and m_N . Generally, λ, k, A , and A_k can be complex. Among them, λ, A and $k A_k$ can be adjusted to be real and positive by redefining the phases of $H_1 H_2$ and N . Thus the tree-level Higgs potential may have at most only one physical phase. It may be chosen to be in $k = k e^{i\alpha}$. This phase may allow for explicit CP violation in the NMSSM. It has been found that the scalar-pseudoscalar mixing in tree-level Higgs potential of the NMSSM stems from either the triple coupling term of the Higgs doublets and the Higgs singlet or the cubic term of the Higgs singlet itself, but not from the coupling between two Higgs doublets [5-7].

In this paper, we impose the restriction of $\alpha = 0$ on the tree-level Higgs potential of the NMSSM. We start with the tree-level Higgs potential which is phase-free, by assuming that λ, k, A , and A_k are real. Thus, $\alpha = 0$ in our tree-level Higgs potential. Now, the two Higgs doublets and the Higgs singlet may be expressed via a unitary transformation as

$$\begin{aligned} H_1 &= \begin{pmatrix} v_1 + S_1 + i \sin A \cos C^+ \\ \sin C^+ \end{pmatrix}; \\ H_2 &= \begin{pmatrix} \cos C^+ \\ v_2 + S_2 + i \cos A \end{pmatrix}; \\ N &= x + X + iY; \end{aligned} \quad (3)$$

where S_1, S_2, X are the scalar Higgs fields, A, Y are the pseudoscalar Higgs fields, and C^+ is the charged Higgs field.

From the tree-level Higgs potential, the symmetric 3×3 mass matrix M_S for the scalar Higgs bosons is obtained in the basis $(S_1; S_2; X)$ as

$$\begin{aligned}
(M_S)_{11} &= m_Z^2 \cos^2 \theta + x(A + kx) \tan \theta ; \\
(M_S)_{22} &= m_Z^2 \sin^2 \theta + x(A + kx) \cot \theta ; \\
(M_S)_{33} &= (2kx)^2 - kxA_k + \frac{v^2 A}{2x} \sin 2\theta ; \\
(M_S)_{12} &= \left(\frac{v^2}{2} - \frac{1}{2} m_Z^2 \right) \sin 2\theta - x(A + kx) ; \\
(M_S)_{13} &= 2 \frac{v^2}{2} x v \cos \theta - v \sin \theta (A + 2kx) ; \\
(M_S)_{23} &= 2 \frac{v^2}{2} x v \sin \theta - v \cos \theta (A + 2kx) ;
\end{aligned} \tag{4}$$

where the gauge boson masses are given as $m_Z^2 = (g_1^2 + g_2^2)v^2 = 2$ and $m_W^2 = g_2^2 v^2 = 2$ for $v = \sqrt{v_1^2 + v_2^2} = 175$ GeV after the electroweak symmetry breaking. In the above mass matrix, the soft SUSY breaking masses $m_{H_1}^2, m_{H_2}^2$, and m_N^2 already are eliminated by minimization conditions with respect to S_1, S_2 , and X . Thus the mass matrix for the scalar Higgs bosons is a function of $\tan \theta = v_2/v_1, A, k, A_k$ and x . The three scalar Higgs boson masses are obtained as

$$m_{S_j}^2 = \frac{1}{3} \text{Tr}(M_S) + 2 \frac{U}{W} \cos \theta - \frac{+ 2j}{3} \quad (j = 1; 2; 3) ; \tag{5}$$

where

$$U = \cos^4 \theta \left[\frac{U}{W^3} \right] ; \tag{6}$$

with

$$\begin{aligned}
W &= \frac{1}{18} f \text{Tr}(M_S) g^2 + \frac{1}{6} \text{Tr}(M_S M_S) ; \\
U &= \frac{5}{108} f \text{Tr}(M_S) g^3 + \frac{1}{12} \text{Tr}(M_S) \text{Tr}(M_S M_S) + \frac{1}{2} \det(M_S) ;
\end{aligned} \tag{7}$$

For the pseudoscalar Higgs bosons, the symmetric 2×2 mass matrix M_P is obtained in the basis $(A; Y)$ as

$$\begin{aligned}
(M_P)_{11} &= \frac{2 x (A + kx)}{\sin 2\theta} ; \\
(M_P)_{22} &= 3kxA_k + 2 kv^2 \sin 2\theta + \frac{v^2}{2x} A \sin 2\theta ; \\
(M_P)_{12} &= v(A - 2kx) ;
\end{aligned} \tag{8}$$

The pseudoscalar Higgs boson masses are given by the eigenvalues of M_P as

$$m_{P_{1,2}}^2 = \frac{1}{2} \left[\text{Tr}(M_P) \pm \sqrt{(\text{Tr}(M_P))^2 - 4 \det(M_P)} \right] ; \tag{9}$$

Finally, the charged Higgs boson mass at the tree level is given as

$$m_C^2 = m_W^2 + \frac{2 x}{\sin 2\theta} (A + kx) ; \tag{10}$$

Unlike in the case of the MSSM, the tree-level mass of the charged Higgs boson can be either heavier or lighter than the W boson according to whether the second is smaller than the third term or not.

Next, we calculate tree-level masses of other relevant fields. These will be used later for evaluating the radiative corrections to the neutral Higgs sector. The fermion matter fields obtain their masses after the electroweak symmetry breaking as $m_t^2 = (h_t v_2)^2$ for top quark, $m_b^2 = (h_b v_1)^2$ for bottom quark, and $m_\tau^2 = (h_\tau v_1)^2$ for tau lepton. The scalar top quarks, the scalar bottom quarks, the scalar tau leptons, and the charginos have their tree-level masses as

$$\begin{aligned}
m_{\tilde{t}_{1,2}}^2 &= m_t^2 + \frac{1}{2}(m_Q^2 + m_T^2) + \frac{m_Z^2}{4} \cos 2\beta - \frac{1}{2}(m_Q^2 - m_T^2) \\
&\quad + \frac{2}{3}m_W^2 - \frac{5}{12}m_Z^2 \cos 2\beta \\
&\quad + m_t^2 (A_t^2 + 2x^2 \cot^2 \beta + 2A_t x \cot \beta \cos \phi_t)^{\frac{1}{2}}; \\
m_{\tilde{b}_{1,2}}^2 &= m_b^2 + \frac{1}{2}(m_Q^2 + m_B^2) - \frac{m_Z^2}{4} \cos 2\beta - \frac{1}{2}(m_Q^2 - m_B^2) \\
&\quad + \frac{1}{12}m_Z^2 - \frac{1}{3}m_W^2 \cos 2\beta \\
&\quad + m_b^2 (A_b^2 + 2x^2 \tan^2 \beta + 2A_b x \tan \beta \cos \phi_b)^{\frac{1}{2}}; \\
m_{\tilde{\nu}_{1,2}}^2 &= m_\tau^2 + \frac{1}{2}(m_L^2 + m_E^2) - \frac{m_Z^2}{4} \cos 2\beta - \frac{1}{2}(m_L^2 - m_E^2) \\
&\quad + \frac{3}{8}m_Z^2 - \frac{1}{2}m_W^2 \cos 2\beta \\
&\quad + m_\tau^2 (A^2 + 2x^2 \tan^2 \beta + 2A x \tan \beta \cos \phi)^{\frac{1}{2}}; \\
m_{\tilde{\nu}_{1,2}}^2 &= \frac{1}{2}(M_2^2 + 2x^2) + m_W^2 - \frac{1}{2}(M_2^2 - 2x^2) - m_W^2 \cos 2\beta \\
&\quad + 2m_W^2 \cos^2 \beta (M_2^2 + 2x^2 \tan^2 \beta + 2M_2 x \tan \beta \cos \phi_c)^{\frac{1}{2}}; \tag{11}
\end{aligned}$$

where $m_Q, m_T, m_B, m_L,$ and m_E are the soft SUSY breaking masses, and $A_t, A_b,$ and A are the trilinear soft SUSY breaking parameters of mass dimension. One can find that there are four phases $\phi_t, \phi_b, \phi,$ and ϕ_c in the above expressions: They are originated from the trilinear soft SUSY breaking parameters A_t, A_b, A and the $SU(2)$ gaugino mass M_2 which are complex in general whereas x is assumed to be real and positive. Note that the scalar fermion masses are not symmetric under $m_Q \leftrightarrow m_T, m_Q \leftrightarrow m_B,$ or $m_L \leftrightarrow m_E$ since D -terms are included in them.

In the NM SSM, there are five neutralinos. Their tree-level masses are obtained from the 5x5 mass matrix

$$\mathbf{M}_{\tilde{\chi}^0} = \begin{pmatrix} 0 & M_1 e^{i\phi_1} & 0 & \frac{g_1}{2} H_1^0 & \frac{g_1}{2} H_2^0 & 0 \\ 0 & 0 & M_2 & \frac{g_2}{2} H_1^0 & \frac{g_2}{2} H_2^0 & 0 \\ \frac{g_1}{2} H_1^0 & \frac{g_2}{2} H_1^0 & 0 & N & H_2^0 & 0 \\ \frac{g_1}{2} H_2^0 & \frac{g_2}{2} H_2^0 & N & 0 & H_1^0 & 0 \\ 0 & 0 & H_2^0 & H_1^0 & 2kN & 0 \end{pmatrix}; \quad (12)$$

where M_1 is the U(1) gaugino mass.

Note that in the above neutralino mass matrix there would appear only one non-trivial phase, which is the relative phase between M_1 and M_2 . We denote it as ϕ_1 . Generally, the neutralino mass matrix may have as much as three phases in the NM SSM. One of them is the same phase as the one associated with the tree-level Higgs potential. Another one of them is identical to the phase, ϕ_c , in the chargino masses. The remaining third phase, ϕ_1 , is essentially associated with the neutral sector, since it is independent of the other sectors in the NM SSM Lagrangian. However, in our case, we have already assumed that μ and k are real. Thus, ϕ_1 is the only one phase in the neutralino mass matrix at the tree level.

The above neutralino mass matrix is complex and symmetric, but not Hermitian. In order to calculate the neutralino masses, the Hermitian matrix $\mathbf{M}_{\tilde{\chi}^0} \mathbf{M}_{\tilde{\chi}^0}^\dagger$ is diagonalized through a similarity transformation. The squared neutralino masses at the tree level are denoted as $m_{\tilde{\chi}^0_i}^2$ ($i = 1$ to 5), and they are sorted such that $m_{\tilde{\chi}^0_i}^2 < m_{\tilde{\chi}^0_j}^2$ for $i < j$. If they are all different from each other, they are obtained as the solutions of

$$\det(\mathbf{M}_{\tilde{\chi}^0} \mathbf{M}_{\tilde{\chi}^0}^\dagger - m_{\tilde{\chi}^0_i}^2 \mathbf{1}_{5 \times 5}) = 0; \quad (13)$$

which may be rewritten as

$$m_{\tilde{\chi}^0_i}^{10} + \tilde{A} m_{\tilde{\chi}^0_i}^8 + \tilde{B} m_{\tilde{\chi}^0_i}^6 + \tilde{C} m_{\tilde{\chi}^0_i}^4 + \tilde{D} m_{\tilde{\chi}^0_i}^2 + \tilde{E} = 0; \quad (14)$$

where the field-dependent \tilde{A} , \tilde{B} , \tilde{C} , \tilde{D} , and \tilde{E} are very complicated and obtainable from Appendix A.

III. Radiative corrections

Now let us consider the radiative corrections. In order to describe the explicit CP violation scenario, it would be convenient to decompose the neutral Higgs fields as

$$\begin{aligned} H_1^0 &= v_1 + h_1 + i \sin \theta_3 h_3; \\ H_2^0 &= v_2 + h_2 + i \cos \theta_3 h_3; \\ N &= x + h_4 + i h_5; \end{aligned} \quad (15)$$

where h_i ($i = 1$ to 5) are the neutral Higgs fields which do not have definite CP parities. In our case with explicit CP violation scenario, they are mixtures of CP-even and CP-odd components. Through radiative corrections, there emerges CP mixing among h_i . On the other hand, the charged Higgs bosons does not mix because both of them are CP-even.

Now, we turn to the radiative corrections. The incomplete cancellation between ordinary particles and their superpartners give the one-loop corrections to the tree-level Higgs boson masses. The full Higgs potential up to the one-loop level is the sum of the tree-level Higgs potential V^0 and the radiative corrections V^1 as

$$V = V^0 + V^1 ;$$

where V^1 may be decomposed into

$$V^1 = V^t + V^b + V + V^{\sim} + V^{\sim 0} ; \quad (16)$$

with superscripts indicate the radiative corrections due to the relevant particles and their superpartners. In fact, the neutral part and the charged one are related to each other. In the NMSSM with explicit CP violation, all the neutral Higgs boson masses can be expressed in terms of the charged Higgs boson mass.

We employ the effective potential method in order to calculate radiative corrections [10]. The general expression for the one-loop effective potential is given by

$$V^1 = \sum_k \frac{c_k}{64\pi^2} (1)^{2J_k} (2J_k + 1) M_k^2 (h_i) g^4 \log \frac{M_k^2 (h_i) g^2}{\mu^2} \frac{3}{2} ;$$

where J_k is the spin of particle or superparticle, μ is the renormalization scale, and $c_k = c_{\text{color}} c_{\text{charge}}$ with c_{color} being the color factor and c_{charge} the charge factor of the corresponding particle or superparticle. We have $c_{\text{color}} = 3$ (1) for colored (uncolored) particles and $c_{\text{charge}} = 2$ (1) for charged (neutral) particles. Note that M_k^2 depends on the neutral Higgs fields h_i ($i = 1$ to 5).

Explicitly, we write down the formulae for the relevant one-loop effective potentials: The one-loop effective potential for the contributions of top quark and scalar top quarks is given by

$$V^t = \sum_{i=1}^3 \frac{X^2}{32\pi^2} \frac{3M_{t_i}^4}{2} \log \frac{M_{t_i}^2}{\mu^2} \frac{3}{2} + \frac{3M_b^4}{16\pi^2} \log \frac{M_b^2}{\mu^2} \frac{3}{2} ;$$

the one for bottom and scalar bottom quarks by

$$V^b = \sum_{i=1}^3 \frac{X^2}{32\pi^2} \frac{3M_{b_i}^4}{2} \log \frac{M_{b_i}^2}{\mu^2} \frac{3}{2} + \frac{3M_b^4}{16\pi^2} \log \frac{M_b^2}{\mu^2} \frac{3}{2} ;$$

the one tau lepton and scalar tau leptons by

$$V = \sum_{i=1}^3 \frac{X^2}{32\pi^2} \frac{M_{\tau_i}^4}{2} \log \frac{M_{\tau_i}^2}{\mu^2} \frac{3}{2} + \frac{M_b^4}{16\pi^2} \log \frac{M_b^2}{\mu^2} \frac{3}{2} ;$$

the one for W boson, the charged Higgs boson, and the charginos by

$$V^{\sim} = \frac{3M_W^4}{32\pi^2} \log \frac{M_W^2}{\mu^2} \frac{3}{2} + \frac{M_{C^+}^4}{32\pi^2} \log \frac{M_{C^+}^2}{\mu^2} \frac{3}{2} + \sum_{i=1}^3 \frac{X^2}{16\pi^2} \frac{M_{\tau_i}^4}{2} \log \frac{M_{\tau_i}^2}{\mu^2} \frac{3}{2} ;$$

and lastly, the one for Z boson, the neutral Higgs bosons and the neutralinos is given by

$$V^{\sim 0} = \frac{3M_Z^4}{64} \log \frac{M_Z^2}{2} + \sum_{i=1}^3 \frac{X^5 M_{h_i}^4}{64} \log \frac{M_{h_i}^2}{2} + \sum_{i=1}^5 \frac{X^5 M_{\tilde{\chi}_i^0}^4}{32} \log \frac{M_{\tilde{\chi}_i^0}^2}{2} + \frac{3}{2} A : \quad (16)$$

Note that in the above one-loop effective potentials fermions enter with a negative sign while bosons with a positive sign.

If CP be conserved in the Higgs sector, h_3 and h_5 would be the pseudoscalar components of the Higgs fields, and the minimum conditions for them would be trivial. In our case of explicit CP violation, the minimum conditions for them are non-trivial. Thus, we obtain two CP-odd tadpole minimum conditions for h_3 and h_5 , respectively, as

$$\begin{aligned} 0 &= \frac{3m_t^2 A_t \sin t}{16^2 v^2 \sin^2 t} f(m_{\tilde{t}_1}^2; m_{\tilde{t}_2}^2) + \frac{3m_b^2 A_b \sin b}{16^2 v^2 \cos^2 b} f(m_{\tilde{b}_1}^2; m_{\tilde{b}_2}^2) \\ &+ \frac{m^2 A \sin}{16^2 v^2 \cos^2} f(m_{\tilde{\tau}_1}^2; m_{\tilde{\tau}_2}^2) + \frac{m^2 M_2 \sin c}{4^2 v^2} f(m_{\tilde{\chi}_1}^2; m_{\tilde{\chi}_2}^2) \\ &+ \sum_{k=1}^8 \frac{X^5 m_{\tilde{\chi}_k^0}^4}{32^2 v^2} \log \frac{m_{\tilde{\chi}_k^0}^2}{2} A_k + \sum_{a \in k} \frac{E_a m_{\tilde{\chi}_k^0}^2}{(m_{\tilde{\chi}_k^0}^2 m_{\tilde{\chi}_a^0}^2)} ; \end{aligned} \quad (17)$$

$$\begin{aligned} 0 &= \frac{3m_t^2 A_t \sin t}{16^2 v \sin^2 t} f(m_{\tilde{t}_1}^2; m_{\tilde{t}_2}^2) + \frac{3m_b^2 A_b \sin b}{16^2 v \cos^2 b} f(m_{\tilde{b}_1}^2; m_{\tilde{b}_2}^2) \\ &+ \frac{m^2 A \sin}{16^2 v \cos^2} f(m_{\tilde{\tau}_1}^2; m_{\tilde{\tau}_2}^2) + \frac{m^2 M_2 \sin c}{4^2 v} f(m_{\tilde{\chi}_1}^2; m_{\tilde{\chi}_2}^2) \\ &+ \sum_{k=1}^8 \frac{X^5 m_{\tilde{\chi}_k^0}^4}{16^2 v \sin^2} \log \frac{m_{\tilde{\chi}_k^0}^2}{2} A_k + \sum_{a \in k} \frac{E_a m_{\tilde{\chi}_k^0}^2}{(m_{\tilde{\chi}_k^0}^2 m_{\tilde{\chi}_a^0}^2)} ; \end{aligned} \quad (18)$$

where the ve terms come respectively from the scalar top quark, the scalar bottom quark, the scalar tau lepton, the chargino, and the neutralino contributions. The dimensionless function arising from radiative corrections is defined by

$$f(m_x^2; m_y^2) = \frac{1}{(m_y^2 - m_x^2)} \left(m_x^2 \log \frac{m_x^2}{2} - m_y^2 \log \frac{m_y^2}{2} \right) + 1 ;$$

and we need to introduce $\tilde{A}_i = (\partial \tilde{A} / \partial h_i)$, $\tilde{B}_i = (\partial \tilde{B} / \partial h_i)$, $\tilde{C}_i = (\partial \tilde{C} / \partial h_i)$, $\tilde{D}_i = (\partial \tilde{D} / \partial h_i)$, and $\tilde{E}_i = (\partial \tilde{E} / \partial h_i)$: In the above minimum conditions, just \tilde{B}_i , \tilde{C}_i , \tilde{D}_i , and \tilde{E}_i ($i = 3$ and 5) enter. Note that no term associated with the tree-level is present in the above minimum conditions since $\tilde{A}_i = 0$.

By differentiating the Higgs potential V at the one-loop level with respect to the neutral Higgs fields, a 5×5 symmetric mass matrix M for them is obtained in the $(h_1; h_2; h_3; h_4; h_5)$ -basis, which may be decomposed as

$$M_{ij} = M_{ij}^0 + M_{ij}^1 ;$$

where M_{ij}^0 is obtained from V^0 while M_{ij}^1 from V^1 . Explicitly, M_{ij}^0 may be expressed in terms of the scalar and pseudoscalar mass matrix elements as to allow M_{ij} be rewritten as

$$M_{11} = (M_S)_{11} + m_A^2 \sin^2 t + M_{11}^1 ;$$

$$\begin{aligned}
M_{22} &= (M_S)_{22} + m_A^2 \cos^2 t + M_{22}^1; \\
M_{33} &= (M_P)_{11} + m_A^2 + M_{33}^1; \\
M_{44} &= (M_S)_{33} + m_B^2 + M_{44}^1; \\
M_{55} &= (M_P)_{22} + m_B^2 + M_{55}^1; \\
M_{12} &= (M_S)_{12} - m_A^2 \cos t \sin t + M_{12}^1; \\
M_{13} &= M_{13}^1; \\
M_{14} &= (M_S)_{13} \frac{m_B^2 x}{v \cos t} + M_{14}^1; \\
M_{15} &= M_{15}^1; \\
M_{23} &= M_{23}^1; \\
M_{24} &= (M_S)_{23} \frac{m_B^2 x}{v \sin t} + M_{24}^1; \\
M_{25} &= M_{25}^1; \\
M_{34} &= M_{34}^1; \\
M_{35} &= (M_P)_{12} + \frac{m_A^2 v \cos t \sin t}{x} + M_{35}^1; \\
M_{45} &= M_{45}^1;
\end{aligned} \tag{19}$$

with $(M_S)_{11} = M_{11}^0$, $(M_S)_{22} = M_{22}^0$, $(M_P)_{11} = M_{33}^0$, $(M_S)_{33} = M_{44}^0$, $(M_P)_{22} = M_{55}^0$, $(M_S)_{12} = M_{12}^0$, $(M_S)_{13} = M_{14}^0$, $(M_S)_{25} = M_{23}^0$, and $(M_P)_{12} = M_{35}^0$. The remaining elements of M_{ij}^0 are explicitly zero since we assume that $\beta = 0$. In Eq (19), we have introduced two expressions for convenience as

$$\begin{aligned}
m_A^2 &= \frac{3m_t^2 A_t x \cos t}{16^2 v^2 \sin^3 t \cos t} f(m_{t_1}^2; m_{t_2}^2) + \frac{3m_b^2 A_b x \cos b}{16^2 v^2 \cos^3 b \sin b} f(m_{b_1}^2; m_{b_2}^2) \\
&+ \frac{m^2 A x \cos t}{16^2 v^2 \cos^3 t \sin t} f(m_{\tilde{t}_1}^2; m_{\tilde{t}_2}^2) + \frac{m_W^2 x M_2 \cos c}{2^2 v^2 \sin^2 c} f(m_{\tilde{t}_1}^2; m_{\tilde{t}_2}^2) \\
&+ \sum_{k=1}^5 \frac{X^5 m_{\tilde{t}_k}^2}{32^2} \log \left[\frac{m_{\tilde{t}_k}^2}{2} A \right] + \frac{A_{33}^8 m_{\tilde{t}_k}^8 + B_{33}^6 m_{\tilde{t}_k}^6 + C_{33}^4 m_{\tilde{t}_k}^4 + D_{33}^2 m_{\tilde{t}_k}^2 + E_{33}}{\mathcal{Q}_k(m_{\tilde{t}_k}^2, m_{\tilde{t}_a}^2)};
\end{aligned}$$

and

$$\begin{aligned}
m_B^2 &= \frac{3m_t^2 A_t \cos t}{16^2 x \tan t} f(m_{t_1}^2; m_{t_2}^2) + \frac{3m_b^2 A_b \cos b}{16^2 x \cot b} f(m_{b_1}^2; m_{b_2}^2) \\
&+ \frac{m^2 A \cos t}{16^2 x \cot t} f(m_{\tilde{t}_1}^2; m_{\tilde{t}_2}^2) + \frac{m_W^2 M_2 \sin^2 c}{8^2 x} f(m_{\tilde{t}_1}^2; m_{\tilde{t}_2}^2) \\
&+ \sum_{k=1}^5 \frac{X^5 m_{\tilde{t}_k}^2}{32^2} \log \left[\frac{m_{\tilde{t}_k}^2}{2} A \right] + \frac{A_{55}^8 m_{\tilde{t}_k}^8 + B_{55}^6 m_{\tilde{t}_k}^6 + C_{55}^4 m_{\tilde{t}_k}^4 + D_{55}^2 m_{\tilde{t}_k}^2 + E_{55}}{\mathcal{Q}_k(m_{\tilde{t}_k}^2, m_{\tilde{t}_a}^2)};
\end{aligned}$$

where in each expression the first term comes from the scalar top quark contributions, the second term from the scalar bottom quarks, the third term from the scalar tau leptons, the fourth one from charginos, and the last term from neutralinos. In m_A and m_B , the coefficients A_{ij} , B_{ij} , C_{ij} , D_{ij} , and E_{ij} ($i = 1$ to 5) are given by $A_{ij} = 5_{ij} A$, $B_{ij} = 5_{ij} B$, $C_{ij} = 5_{ij} C$, $D_{ij} = 5_{ij} D$, and $E_{ij} = 5_{ij} E$, where the second-order differential operator is defined as

$$5_{ij} = \frac{\partial^2}{\partial h_i \partial h_j} - \frac{1}{v_1} \frac{\partial}{\partial h_1} \delta_{ij} - \frac{1}{v_2} \frac{\partial}{\partial h_2} \delta_{ij} - \frac{\sin^2 t}{v_1} \frac{\partial}{\partial h_1} + \frac{\cos^2 t}{v_2} \frac{\partial}{\partial h_2} \delta_{ij}$$

$$\frac{1}{x} \frac{\partial}{\partial h_4} \Big|_{4j} - \frac{1}{x} \frac{\partial}{\partial h_4} \Big|_{5j} ; \quad (20)$$

for $j = i$ ($i, j = 1$ to 5). In the above differential operator, all the terms except the first one are caused by the shift in the vacuum due to the radiative corrections.

We may further decompose M_{ij}^1 as

$$M_{ij}^1 = M_{ij}^t + M_{ij}^b + M_{ij} + M_{ij}^{\sim} + M_{ij}^{\sim 0} ;$$

where M_{ij}^t is obtained from V^t , M_{ij}^b from V^b , M_{ij} from V , M_{ij}^{\sim} from V^{\sim} , and $M_{ij}^{\sim 0}$ from $V^{\sim 0}$, after imposing the CP-odd tadpole minimum conditions for h_3 and h_5 . We note that M_{ij}^{\sim} and $M_{ij}^{\sim 0}$ are matrices for squared masses. The elements of M_{ij}^{\sim} have no colour factor. In Appendix B are presented the complicated formulae for M_{ij}^t . In Appendix C for M_{ij}^b , in Appendix D for M_{ij} , and in Appendix E for M_{ij}^{\sim} .

Now, we concentrate on $M_{ij}^{\sim 0}$, which represents the radiative corrections due to the contributions from the neutralino sector: It consists of the contributions from Z boson, tree-level scalar and pseudoscalar Higgs bosons, and neutralinos. Thus, we may decompose it further again as

$$M_{ij}^{\sim 0} = M_{ij}^Z + M_{ij}^S + M_{ij}^P + M_{ij}^{\tilde{\chi}^0}$$

where each term represents the relevant contribution. Let us describe one by one.

The contribution of Z boson affects the four elements $M_{11}^{\sim 0}$, $M_{22}^{\sim 0}$, and $M_{12}^{\sim 0} = M_{21}^{\sim 0}$ only, since the Higgs singlet N does not couple to Z boson. Calculations yield the contribution of Z boson as

$$\begin{pmatrix} 0 & 1 \\ B_{11}^Z & C_{12}^Z \\ B_{22}^Z & C_{21}^Z \\ B_{12}^Z & C_{11}^Z \end{pmatrix} = \begin{pmatrix} 0 & 1 \\ B_{11}^{\cos^2} & C_{12}^{\cos \sin} \\ B_{22}^{\sin^2} & C_{21}^{\cos \sin} \\ B_{12}^{\cos \sin} & C_{11}^{\cos \sin} \end{pmatrix} - \frac{3m_Z^4}{16\sqrt{2}} \log \frac{m_Z^2}{2} ; \quad (21)$$

with $B_{21}^Z = B_{12}^Z$.

The contribution of the tree-level scalar Higgs bosons is obtained as

$$M_{ij}^S = \sum_{l=1}^3 \frac{X^3}{64} \frac{m_{S_l}^2}{2} \log \frac{m_{S_l}^2}{2} - \sum_{l=1}^3 \frac{\partial^2 m_{S_l}^2}{\partial h_i \partial h_j} + \sum_{l=1}^3 \frac{X^3 \log(m_{S_l}^2 = 2)}{64} \frac{\partial m_{S_l}^2}{\partial h_i} \frac{\partial m_{S_l}^2}{\partial h_j} ; \quad (22)$$

where $m_{S_l}^2$ ($l = 1, 2, 3$) are the tree-level masses of the scalar Higgs bosons of Eq. (5), and

$$\frac{\partial m_{S_a}^2}{\partial h_i} = \frac{A_i m_{S_a}^4 + B_i m_{S_a}^2 + C_i}{(m_{S_a}^2 - m_{S_b}^2)(m_{S_a}^2 - m_{S_c}^2)} ; \quad (23)$$

and

$$\begin{aligned} \frac{\partial^2 m_{S_a}^2}{\partial h_i \partial h_j} = & \frac{(5_{ij} A) m_{S_a}^4 + (5_{ij} B) m_{S_a}^2 + (5_{ij} C)}{(m_{S_a}^2 - m_{S_b}^2)(m_{S_a}^2 - m_{S_c}^2)} \\ & + \frac{1}{(m_{S_a}^2 - m_{S_b}^2)} \frac{\partial m_{S_a}^2}{\partial h_i} \frac{\partial m_{S_b}^2}{\partial h_j} + \frac{\partial m_{S_b}^2}{\partial h_i} \frac{\partial m_{S_a}^2}{\partial h_j} \\ & + \frac{1}{(m_{S_a}^2 - m_{S_c}^2)} \frac{\partial m_{S_a}^2}{\partial h_i} \frac{\partial m_{S_c}^2}{\partial h_j} + \frac{\partial m_{S_c}^2}{\partial h_i} \frac{\partial m_{S_a}^2}{\partial h_j} ; \end{aligned} \quad (24)$$

for $i = 1$ to 5 , and $m_{S_a}^2 \in m_{S_b}^2 \in m_{S_c}^2$. Here, we introduce

$$\begin{aligned} A &= \text{Tr}(M_S); \\ B &= M_{S_{11}} M_{S_{22}} + M_{S_{11}} M_{S_{33}} + M_{S_{22}} M_{S_{33}} + M_{S_{12}}^2 + M_{S_{23}}^2 + M_{S_{13}}^2; \\ C &= \det(M_S); \end{aligned} \quad (25)$$

where $M_{S_{ij}}$ are given in Appendix F, and $A_i = (\partial A / \partial h_i)$, $B_i = (\partial B / \partial h_i)$, and $C_i = (\partial C / \partial h_i)$.

As aforementioned, all terms in 5_{ij} except the first one are caused by the shifts in the vacuum due to the radiative corrections. Note that the shifts take place along h_1, h_2 , and h_4 . Those shifts occur actually on only the diagonal elements of the mass matrix of the neutral Higgs boson through 5_{ij} : M_{11} by the second term of 5 , M_{22} by the third term, M_{33} by the fourth term, M_{44} by the fifth term, and M_{55} by the sixth term, respectively. Since the tree-level Higgs potential does not possess the scalar-pseudoscalar mixing, both h_3 and h_5 become the pseudoscalar Higgs fields and $\langle V \rangle = \langle h_3 \rangle = \langle h_5 \rangle = 0$. At the one-loop level the non-trivial solutions for h_3 and h_5 already are obtained by the CP-odd tadpole minimum conditions.

Next, the contribution of the tree-level pseudoscalar Higgs bosons is obtained as

$$\begin{aligned} P_{ij} &= \frac{(5_{ij} A_P)}{64^2} \left(m_{P_1}^2 \log \frac{m_{P_1}^2}{2} + m_{P_2}^2 \log \frac{m_{P_2}^2}{2} \right) \\ &+ \frac{1}{64^2} \frac{\partial A_P}{\partial h_i} \frac{\partial A_P}{\partial h_j} + \frac{\partial A_P}{\partial h_j} \frac{\partial W_P}{\partial h_i} \frac{\log(m_{P_1}^2 - m_{P_2}^2)}{(m_{P_1}^2 - m_{P_2}^2)} - \frac{(5_{ij} W_P)}{64^2} f(m_{P_1}^2; m_{P_2}^2) \\ &+ \frac{1}{64^2} \frac{\partial W_P}{\partial h_i} \frac{\partial W_P}{\partial h_j} \frac{g(m_{P_1}^2; m_{P_2}^2)}{(m_{P_1}^2 - m_{P_2}^2)^2} + \frac{1}{64^2} \frac{\partial A_P}{\partial h_i} \frac{\partial A_P}{\partial h_j} \log \frac{m_{P_1}^2 m_{P_2}^2}{4}, \end{aligned} \quad (26)$$

for $i, j = 1$ to 5 , and $m_{P_1}^2$ and $m_{P_2}^2$ are the tree-level masses of pseudoscalar Higgs bosons. Here, we have introduced A_P and W_P as

$$\begin{aligned} A_P &= \frac{(M_{P_{44}} + M_{P_{55}})}{2}; \\ W_P &= \frac{(M_{P_{44}} - M_{P_{55}})^2}{4} + M_{P_{45}}^2; \end{aligned} \quad (27)$$

where $M_{P_{ij}}$ are given in Appendix G.

Lastly, the contribution of the neutralinos is obtained as

$$N_{ij}^0 = \sum_{i=1}^5 \frac{m_{\tilde{1}}^2}{32^2} \frac{\partial \log \frac{m_{\tilde{1}}^2}{2}}{\partial h_i} \frac{\partial \log \frac{m_{\tilde{1}}^2}{2}}{\partial h_j} + \sum_{i=1}^5 \frac{1}{32^2} \log \frac{m_{\tilde{1}}^2}{2} \frac{\partial m_{\tilde{1}}^2}{\partial h_i} \frac{\partial m_{\tilde{1}}^2}{\partial h_j} : \quad (28)$$

where

$$\frac{\partial m_a^2}{\partial h_i} = \frac{A_i m_a^8 + B_i m_a^6 + C_i m_a^4 + D_i m_a^2 + E_i}{(m_a^2 - m_b^2)(m_a^2 - m_c^2)(m_a^2 - m_d^2)(m_a^2 - m_e^2)}; \quad (29)$$

and

$$\begin{aligned} \frac{\partial^2 m_a^2}{\partial h_i \partial h_j} &= \frac{A_{ij} m_a^8 + B_{ij} m_a^6 + C_{ij} m_a^4 + D_{ij} m_a^2 + E_{ij}}{(m_a^2 - m_b^2)(m_a^2 - m_c^2)(m_a^2 - m_d^2)(m_a^2 - m_e^2)} \\ &+ \frac{1}{(m_a^2 - m_b^2)} \frac{\partial m_a^2}{\partial h_i} \frac{\partial m_b^2}{\partial h_j} + \frac{\partial m_b^2}{\partial h_i} \frac{\partial m_a^2}{\partial h_j} \\ &+ \frac{1}{(m_a^2 - m_c^2)} \frac{\partial m_a^2}{\partial h_i} \frac{\partial m_c^2}{\partial h_j} + \frac{\partial m_c^2}{\partial h_i} \frac{\partial m_a^2}{\partial h_j} \end{aligned}$$

$$\begin{aligned}
& + \frac{1}{(m_a^2 - m_d^2)} \frac{\partial m_a^2}{\partial h_i} \frac{\partial m_d^2}{\partial h_j} + \frac{\partial m_d^2}{\partial h_i} \frac{\partial m_a^2}{\partial h_j} \\
& + \frac{1}{(m_a^2 - m_e^2)} \frac{\partial m_a^2}{\partial h_i} \frac{\partial m_e^2}{\partial h_j} + \frac{\partial m_e^2}{\partial h_i} \frac{\partial m_a^2}{\partial h_j} :
\end{aligned} \tag{30}$$

for $i, j = 1$ to 5 . In the above two expressions, we use the shorthand notations for the neutralino masses: $m_a^2 = m_{\tilde{\chi}_0^0}$ and so on. We assume that none of the neutralino masses are equal one another.

We note that \tilde{m}_{ij}^0 in above equation is not in its final form, in the sense that the two CP-odd tadpole minimum conditions should be applied to obtain the explicit results. The minimum conditions on h_1, h_2 , and h_4 are already imposed through the differential operators ∂_{ij} .

IV. Numerical Results

Now, let us analyze numerically the radiative corrections to the neutral Higgs boson masses at the one-loop level in the NMSSM. In the NMSSM without explicit CP violation scenario, it is known that a massless scalar Higgs boson might exist without contradicting the experimental failure to discover any scalar Higgs boson at LEP2 [9]. The massless scalar Higgs boson is essentially possible in the NMSSM not because of CP phases but because of the Higgs singlet in the model. Actually, in the NMSSM, the lightest scalar Higgs boson has a small coupling to Z boson pair due to the Higgs singlet, which makes the production cross section for it through Higgs-strahlung process very small. On the other hand, in the MSSM without explicit CP violation, a large range of the mass of the lightest scalar Higgs boson is excluded by the LEP2 data.

If CP symmetry be conserved in the Higgs sector of the NMSSM, the ν Higgs fields decouple such that h_1, h_2 , and h_4 would become the scalar Higgs bosons while h_3 and h_5 the pseudoscalar Higgs bosons. There would be no mixing between them. The CP violation is dictated by the six off-diagonal elements of the mass matrix, $M_{13}, M_{23}, M_{34}, M_{15}, M_{25}$, and M_{45} , of the neutral Higgs bosons in the basis $(h_1; h_2; h_3; h_4; h_5)$, which describe the scalar-pseudoscalar mixing. The remaining off-diagonal elements describe the scalar-scalar mixing or the pseudoscalar-pseudoscalar mixing, and have nothing to do with the CP violation.

For numerical analysis, we set the fermion masses as $m_t = 175$ GeV, $m_b = 4$ GeV, and $m_c = 1.7$ GeV, the gauge boson masses as $m_Z = 91.1$ GeV and $m_W = 80.4$ GeV, and the weak mixing angle as $\sin^2 \theta_W = 0.23$. In the one-loop effective potential, the renormalization scale is set as $\mu = 300$ GeV. By assuming universal gaugino masses at GUT scale, the low-energy values of the U(1) and SU(2) gaugino masses has a mass relation of $M_1 = 5/3 \tan^2 \theta_W M_2$. To be specific, we take a representative point in the parameter space: We choose $\beta = k = 0.3$, $A = 300$ GeV, $A_k = 200$ GeV, $x = A_t = A_b = A_c = 900$ GeV, $m_Q = m_L = M_2 = 800$ GeV, and $m_T = m_B = m_E = 400$ GeV. The complex phases except the one from neutralino contributions are fixed as $\phi_t = \phi_b = \phi_c = 8 = 5$. Then, we are left essentially with two free parameters: ϕ_1 and $\tan \beta$. The phase ϕ_1 from the neutralino contributions is allowed to vary as $0 < \phi_1 < 2\pi$, and $\tan \beta$ is set to vary within 2 and 40.

With these specific numbers as input, Figs 1a and 1b show the numerical results for the six mixing elements of the scalar-pseudoscalar Higgs boson, $M_{13}, M_{23}, M_{34}, M_{15}, M_{25}$, and M_{45} , at the one-loop level, as functions of ϕ_1 , and $\tan \beta = 10$. The unit is $(\text{GeV})^2$. In Fig 1a, three curves for M_{13} (solid curve), M_{23} (dashed curve), and M_{34} (dotted curve) are displayed, while in Fig. 1b for M_{15} (solid curve), M_{25} (dashed curve), M_{45} (dotted curve). Our analysis indicates

that for a particular choice of parameters in the NMSSM with explicit CP violation, the scalar-pseudoscalar mixing can significantly be modified by the one-loop neutralino contribution. Note that a similar behavior is observed in the MSSM: A scalar-pseudoscalar mixing element may increase as much as twice the neutralino contribution as the relevant phase varies from 0 to 2π [3]. We find that the dependence on β_1 of all the neutral Higgs boson masses are very weak. For Figs. 1a and 1b, we obtain m_{h_i} ($i = 1, 2, 3, 4, 5$) = 122, 401, 491, 1243, and 1252 GeV. If the Higgs sector has not any CP phase, among the elements O_{ij} ($i, j = 1$ to 5) of the transformation matrix which diagonalize the neutral Higgs boson mass matrix, $O_{13}, O_{23}, O_{34}, O_{15}, O_{25}$, and O_{45} are all zero. In Fig. 1c and 1d, we plot them, as a function of the CP phase, for the same as Fig. 1a. The elements O_{13}^2, O_{15}^2 , and O_{45}^2 suffer a large fluctuation, while the remaining ones are almost stable.

In Fig. 2a, we present the results for the mass of the lightest neutral Higgs boson as a function of β_1 , for some values of $\tan\beta$. Four curves are shown for $\tan\beta = 2$ (solid curve), $\tan\beta = 10$ (dashed curve), $\tan\beta = 25$ (dotted curve), and $\tan\beta = 40$ (dot-dashed curve). It can be observed that the mass of the lightest neutral Higgs boson varies very weakly as β_1 varies. The dependence on $\tan\beta$ of the mass of the lightest neutral Higgs boson is not so clear. As $\tan\beta$ increases, the lightest neutral Higgs boson becomes heavier first until $\tan\beta = 10$ but then its mass decreases. This is different from the case of the MSSM. In the MSSM, the lightest neutral Higgs boson mass increases steadily as $\tan\beta$ increases.

The lightest neutral Higgs boson mass does not increase in accordance with the increase of $\tan\beta$, because of the Higgs singlet in the NMSSM. One can see that in Fig. 2a the lightest neutral Higgs boson mass becomes maximum around $\beta_1 = \beta_1^*$ for $2 < \tan\beta < 40$. Nevertheless, the lightest neutral Higgs boson mass is shown to be relatively independent of the variation in β_1 . Also, we find that the masses of the remaining four neutral Higgs bosons, as functions of β_1 , remain almost unchanged: Their changes are less than 5% for $0 < \beta_1 < 2\pi$. This behavior is similar with the mass of the lightest neutral Higgs boson in the MSSM, with explicit CP violation. In the MSSM with explicit CP violation, it is found that, against the change of the relevant phase for the neutralino contributions from 0 to 2π , the lightest neutral Higgs boson mass is roughly stable [4] whereas the scalar-pseudoscalar mixing elements change significantly [3, 4]. In Fig. 2b, we calculate the lightest neutral Higgs boson mass, as a function of μ , for the same as Fig. 2a, except for $\beta_1 = 3\pi/5$. The lightest neutral Higgs boson mass is dependent on the renormalization scale even though its dependence is weak. Physical observable quantities, for example, the lightest neutral Higgs boson mass should be scale-independent. Since we consider only the one-loop correction, the lightest neutral Higgs boson mass is dependent on the scale. If more higher contributions are considered, the dependence would be weakly.

The scalar-pseudoscalar mixing, which is responsible for CP violation in the NMSSM, is triggered by ν phases. The size of the mixing can be regarded as maximal if $\sin(\nu_t) = \sin(\nu_b) = \sin(\nu_c) = \sin(\nu_s) = \sin(\nu_1) = 1$, and minimal if $\sin(\nu_t) = \sin(\nu_b) = \sin(\nu_c) = \sin(\nu_s) = \sin(\nu_1) = 0$. The minimal mixing implies $M_{13} = M_{23} = M_{34} = M_{15} = M_{25} = M_{45} = 0$, and the mixing disappears to restore the CP symmetry. Meanwhile, one can evaluate effectively the size of the CP violation by measuring the dimensionless parameter [6]

$$= 5^5 O_{11}^2 O_{21}^2 O_{31}^2 O_{41}^2 O_{51}^2 ;$$

where O_{ij} ($i, j = 1$ to 5) are the elements of the orthogonal transformation matrix that diagonalizes the neutral Higgs boson mass matrix. The range of ν is from 0 to 1 since the elements of the transformation matrix satisfy the orthogonality condition of $\sum_{j=1}^5 O_{j1}^2 = 1$. If $\nu = 0$, there is no explicit CP violation in the Higgs sector of the NMSSM. On the other hand, if $\nu = 1$,

CP symmetry is maximally violated through the scalar-pseudoscalar mixing. The maximal CP violation that leads to $\theta = 1$ takes place when $O_{11}^2 = O_{21}^2 = O_{31}^2 = O_{41}^2 = O_{51}^2 = 1/5$. The elements O_{ij} determine the couplings of the physical neutral Higgs bosons to the other states in the NMSSM.

In Figure 3, we show θ as a function of $\tan \beta$, for two representative values of μ_1 . The solid curve is obtained for $\mu_1 = \mu = 5$ and the dashed curve for $\mu_1 = 3\mu = 15$ in Figure 3. The remaining parameters are the same as other figures. One can observe that the scalar-pseudoscalar mixing decreases quite quickly as $\tan \beta$ increases from 2 to 40 for both of the curves.

Up to now, our analysis is carried out for a specific set of parameter values (except μ_1). Thus, the results in Figs 1-3 might not faithfully represent the whole parameter space of the the NMSSM. In order to obtain a more comprehensive view over how the scalar-pseudoscalar mixing elements and the lightest neutral Higgs boson mass depend on various parameters, we have to explore the parameter space in more detail.

A point in the parameter space is naturally a given set of parameter values. Within the parameter space whose boundaries are defined by

$$\begin{aligned} \mu &= 300 \text{ GeV} \\ 0 < m_t = m_b = m_c < 2 \\ 2 < \tan \beta < 40 \\ 0 < \mu_1; k < 0.7 \\ 0 < A_k; A_k; x; M_2 < 1000 \text{ GeV} \\ 0 < A_t = A_b = A_c < 1000 \text{ GeV} \\ 0 < m_Q = m_L < 1000 \text{ GeV} \\ 0 < m_T = m_B = m_E < 1000 \text{ GeV} \end{aligned}$$

and

$$0 < \mu_1 < 2 : \quad :$$

We choose 40,000 points for investigation in the following way.

Using the Monte Carlo method, we first choose a point in the parameter space. Then, by changing the parameter values other than μ_1 , we pick up randomly the value of μ_1 to choose another point. These two points have therefore equal parameter values except for the value of μ_1 . We check for each of the two points if the condition of $m_{h_{(n+1)}} - m_{h_{(n)}} > 10 \text{ GeV}$, ($n = 1$ to 4) is satisfied. If so, we keep them and group them into a pair of points, in order to compare the effects of μ_1 . In this way, we select 20,000 pairs of points.

Let the values of μ_1 of a given pair of the two points be c_1 and c_2 . We define R_1 and R_{ij} ($i; j = 1$ to 5) by

$$R_1 = \frac{c_1}{c_2} \text{ and } R_{ij} = \frac{M_{ij}(\mu_1 = c_1)}{M_{ij}(\mu_1 = c_2)}$$

for $M_{ij}(\mu_1 = c_1) > M_{ij}(\mu_1 = c_2)$ and

$$R_1 = \frac{c_2}{c_1} \text{ and } R_{ij} = \frac{M_{ij}(\mu_1 = c_2)}{M_{ij}(\mu_1 = c_1)}$$

for $M_{ij}(\mu_1 = c_1) < M_{ij}(\mu_1 = c_2)$. In this way, we can make $R_{ij} \geq 1$ for any R_1 . In Figures 4a-4f, we plot $R_{13}, R_{23}, R_{34}; R_{15}, R_{25},$ and R_{45} , respectively, against R_1 . If $R_{ij} = 1$, regardless of R_1 , it implies that there is no effect of μ_1 , or that there is no contribution of the neutralinos

to the scalar-pseudoscalar mixing. One can observe that all of R_{ij} exhibit large deviations from 1 for most of the parameter space. Those figures assure us that the significance of the neutralino contributions are actually not a peculiar behavior of a specific choice of parameter values but widely common for a large number of points in the parameter space. For a large part of the parameter space, it is rather safe to expect that the neutralino contributions to the scalar-pseudoscalar mixing are relatively dominant.

We repeat the above procedure with another 20,000 set of two points in the parameter space. Here, we define R_1 and R_{hi} ($i = 1$ to 5) by

$$R_1 = \frac{c_1}{c_2} \text{ and } R_{hi} = \frac{m_{h_i}(\mu = c_1)}{m_{h_i}(\mu = c_2)}$$

for $m_{h_i}(\mu = c_1) > m_{h_i}(\mu = c_2)$, and

$$R_1 = \frac{c_2}{c_1} \text{ and } R_{hi} = \frac{m_{h_i}(\mu = c_2)}{m_{h_i}(\mu = c_1)}$$

for $m_{h_i}(\mu = c_1) < m_{h_i}(\mu = c_2)$. The difference from the previous case is that we obtain in this case the Higgs masses explicitly.

In Fig 5, we plot R_{h1} against R_1 . Here, $R_{h1} = 1$ implies that the lightest neutral Higgs boson mass is independent of the neutralino contributions. One can see in Fig 5 that most of the points are around the line of $R_{h1} = 1$. This implies that the portion of the parameter space which exhibit nonnegligible neutralino contributions to the lightest neutral Higgs boson mass is small.

V. Conclusions

We have investigated the possibility of explicit CP violation at the one-loop level in the neutral Higgs sector of the NMSSM, where the tree-level Higgs potential is assumed to possess CP symmetry. The mixing between the scalar and pseudoscalar Higgs bosons, which induce the CP violation, occurs via the radiative corrections at the one-loop level. For the radiative corrections, we consider the loop contributions due to top quark, bottom quark, tau lepton, W boson, Z boson, the charged Higgs boson, the neutral Higgs bosons and their superpartners. With those contributions, new phases appear. They are: ϕ_t from the scalar top quark masses, ϕ_b from the scalar bottom quark masses, ϕ_τ from the tau lepton masses, ϕ_c from the chargino masses, and ϕ_1 from the neutralino masses. We pay attention to ϕ_1 .

For a wide parameter space of the NMSSM, we consider the scalar-pseudoscalar mixing and the mass of the lightest neutral Higgs boson. We find that the scalar-pseudoscalar mixing are affected relatively largely by the neutralino contribution via the phase ϕ_1 . The mixing elements between scalar and pseudoscalar Higgs fields in the basis of $(h_1; h_2; h_3; h_4; h_5)$ fluctuates strongly as ϕ_1 is changed from 0 to 2π . Meanwhile, the mass of the lightest neutral Higgs boson is found to be relatively stable for $0 < \phi_1 < 2\pi$. Concludingly, we find that the neutralino contributions at the one-loop level to the scalar-pseudoscalar mixing in the NMSSM with explicit CP violation exhibit relatively significant effects.

Acknowledgments

This work was supported by Korea Research Foundation Grant (2001-050-D 00005).

Appendix A

The elements for the field-dependent mass matrix $M_{\tilde{\nu}_i \tilde{\nu}_j}^0$ of the neutralinos at the tree level are

$$\begin{aligned}
 M_{\tilde{\nu}_1 \tilde{\nu}_1}^0 &= \frac{g_1^2}{2} \mathcal{H}_1^0 \mathcal{J}^2 + \mathcal{H}_2^0 \mathcal{J}^2 + \frac{1}{4} M_2^2 ; \\
 M_{\tilde{\nu}_2 \tilde{\nu}_2}^0 &= \frac{g_2^2}{2} \mathcal{H}_1^0 \mathcal{J}^2 + \mathcal{H}_2^0 \mathcal{J}^2 + M_2^2 ; \\
 M_{\tilde{\nu}_3 \tilde{\nu}_3}^0 &= \frac{1}{2} g_1^2 + g_2^2 \mathcal{H}_1^0 \mathcal{J}^2 + \mathcal{N}^2 \mathcal{J}^2 + \mathcal{H}_2^0 \mathcal{J}^2 ; \\
 M_{\tilde{\nu}_4 \tilde{\nu}_4}^0 &= \frac{1}{2} g_1^2 + g_2^2 \mathcal{H}_2^0 \mathcal{J}^2 + \mathcal{N}^2 \mathcal{J}^2 + \mathcal{H}_1^0 \mathcal{J}^2 ; \\
 M_{\tilde{\nu}_5 \tilde{\nu}_5}^0 &= 4k^2 \mathcal{N}^2 \mathcal{J}^2 + \mathcal{H}_1^0 \mathcal{J}^2 + \mathcal{H}_2^0 \mathcal{J}^2 ; \\
 M_{\tilde{\nu}_1 \tilde{\nu}_2}^0 &= \frac{g_1 g_2}{2} \mathcal{H}_1^0 \mathcal{J}^2 + \mathcal{H}_2^0 \mathcal{J}^2 ; \\
 M_{\tilde{\nu}_1 \tilde{\nu}_3}^0 &= \frac{g_1}{2} \mathcal{H}_2^0 \mathcal{N} + \mathcal{H}_1^0 M_1 e^{i\beta} ; \\
 M_{\tilde{\nu}_1 \tilde{\nu}_4}^0 &= \frac{g_1}{2} \mathcal{H}_1^0 \mathcal{N} + \mathcal{H}_2^0 M_1 e^{i\beta} ; \\
 M_{\tilde{\nu}_1 \tilde{\nu}_5}^0 &= \frac{g_1}{2} \mathcal{H}_1^0 \mathcal{H}_2^0 + \mathcal{H}_1^0 \mathcal{H}_2^0 ; \\
 M_{\tilde{\nu}_2 \tilde{\nu}_3}^0 &= \frac{g_2}{2} \mathcal{H}_1^0 M_2 + \mathcal{N} \mathcal{H}_2^0 ; \\
 M_{\tilde{\nu}_2 \tilde{\nu}_4}^0 &= \frac{g_2}{2} \mathcal{H}_2^0 M_2 + \mathcal{N} \mathcal{H}_1^0 ; \\
 M_{\tilde{\nu}_2 \tilde{\nu}_5}^0 &= \frac{g_2}{2} \mathcal{H}_1^0 \mathcal{H}_2^0 + \mathcal{H}_1^0 \mathcal{H}_2^0 ; \\
 M_{\tilde{\nu}_3 \tilde{\nu}_4}^0 &= \frac{1}{2} g_1^2 + g_2^2 \mathcal{H}_1^0 \mathcal{H}_2^0 + \mathcal{H}_1^0 \mathcal{H}_2^0 ; \\
 M_{\tilde{\nu}_3 \tilde{\nu}_5}^0 &= \mathcal{N} \mathcal{H}_1^0 + 2k \mathcal{N} \mathcal{H}_2^0 ; \\
 M_{\tilde{\nu}_4 \tilde{\nu}_5}^0 &= \mathcal{N} \mathcal{H}_2^0 + 2k \mathcal{N} \mathcal{H}_1^0 ; \tag{31}
 \end{aligned}$$

Appendix B

The elements for the mass matrix of the neutral Higgs bosons due to the radiative contributions of the top quark and scalar top quarks are

$$\begin{aligned}
 M_{11}^t &= \frac{3}{8} \frac{m_t^2}{2v^2} \frac{x_{t_1}}{\sin \tau} + \frac{\cos \tau}{2} \frac{g(m_{t_1}^2; m_{t_2}^2)}{(m_{t_2}^2 - m_{t_1}^2)^2} + \frac{3m_Z^4 \cos^2 \tau}{128} \frac{\log \frac{m_{t_1}^2 m_{t_2}^2}{4}}{2v^2} \\
 &\quad + \frac{3 \cos^2 \tau}{16} \frac{4m_W^2}{3} \frac{5m_Z^2}{6} f(m_{t_1}^2; m_{t_2}^2) \\
 &\quad + \frac{3m_Z^2 \cos \tau}{16} \frac{m_t^2}{2v^2} \frac{x_{t_1}}{\sin \tau} + \frac{\cos \tau}{2} \frac{\log(m_{t_2}^2 - m_{t_1}^2)}{(m_{t_2}^2 - m_{t_1}^2)} ;
 \end{aligned}$$

$$\begin{aligned}
M_{22}^t &= \frac{3}{8} \frac{m_t^2 A_t}{2v^2} \frac{\sin t}{\sin^2} \frac{g(m_{t_1}^2; m_{t_2}^2)}{(m_{t_2}^2 - m_{t_1}^2)^2} \frac{3m_t^4}{4} \frac{\log \frac{m_t^2}{2}}{2v^2 \sin^2} \\
&\quad + \frac{3 \sin^2}{16} \frac{4m_t^2}{2v^2} \frac{5m_t^2}{6} f(m_{t_1}^2; m_{t_2}^2) \\
&\quad + \frac{3 \sin}{16} \frac{4m_t^2}{2v^2} \frac{m_t^2}{\sin^2} \frac{m_t^2 A_t}{\sin} \frac{\sin t}{2} \frac{\log(m_{t_2}^2 = m_{t_1}^2)}{(m_{t_2}^2 - m_{t_1}^2)} \\
&\quad + \frac{3}{32} \frac{2m_t^2}{2v^2} \frac{m_t^2 \sin}{\sin} \frac{\log \frac{m_{t_1}^2 m_{t_2}^2}{4}}{2} ;
\end{aligned}$$

$$M_{33}^t = \frac{3m_t^4 A_t^2 x^2 \sin^2 t}{8} \frac{g(m_{t_1}^2; m_{t_2}^2)}{2v^2 \sin^4 (m_{t_2}^2 - m_{t_1}^2)^2} ;$$

$$M_{44}^t = \frac{3m_t^4 x^2}{8} \frac{g(m_{t_1}^2; m_{t_2}^2)}{2 \tan^2 (m_{t_2}^2 - m_{t_1}^2)^2} ;$$

$$M_{55}^t = \frac{3m_t^4 A_t^2 \sin^2 t}{8} \frac{g(m_{t_1}^2; m_{t_2}^2)}{2 \tan^2 (m_{t_2}^2 - m_{t_1}^2)^2} ;$$

$$\begin{aligned}
M_{12}^t &= \frac{3}{8} \frac{m_t^2 x}{2v^2} \frac{\cos t}{\sin} + \frac{\cos t}{2} \frac{m_t^2 A_t}{\sin} \frac{\sin t}{2} \frac{g(m_{t_1}^2; m_{t_2}^2)}{(m_{t_2}^2 - m_{t_1}^2)^2} \\
&\quad + \frac{3 \sin 2}{32} \frac{4m_t^2}{2v^2} \frac{5m_t^2}{6} f(m_{t_1}^2; m_{t_2}^2) \\
&\quad + \frac{3 \sin}{32} \frac{4m_t^2}{2v^2} \frac{m_t^2 x}{\sin^2} + \frac{\cos t}{2} \frac{\log(m_{t_2}^2 = m_{t_1}^2)}{(m_{t_2}^2 - m_{t_1}^2)} \\
&\quad + \frac{3m_t^2 \cos}{32} \frac{m_t^2 A_t}{2v^2} \frac{\sin t}{\sin} \frac{\log(m_{t_2}^2 = m_{t_1}^2)}{2 (m_{t_2}^2 - m_{t_1}^2)} \\
&\quad + \frac{3m_t^2 \sin 2}{256} \frac{4m_t^2}{2v^2} \frac{m_t^2}{\sin^2} \log \frac{m_{t_1}^2 m_{t_2}^2}{4} ;
\end{aligned}$$

$$\begin{aligned}
M_{13}^t &= \frac{3m_t^2 A_t x \sin t}{8} \frac{m_t^2 x}{2v^2 \sin^2} + \frac{\cos t}{2} \frac{g(m_{t_1}^2; m_{t_2}^2)}{(m_{t_2}^2 - m_{t_1}^2)^2} \\
&\quad + \frac{3m_t^2 m_t^2 A_t x \sin t}{32} \frac{\log(m_{t_2}^2 = m_{t_1}^2)}{2v^2 \sin \tan (m_{t_2}^2 - m_{t_1}^2)} ;
\end{aligned}$$

$$\begin{aligned}
M_{14}^t &= \frac{3m_t^2}{8} \frac{m_t^2 x}{2v \tan} \frac{\cos t}{\sin} + \frac{\cos t}{2} \frac{g(m_{t_1}^2; m_{t_2}^2)}{(m_{t_2}^2 - m_{t_1}^2)^2} \frac{3m_t^2 x \cot}{8} \frac{f(m_{t_1}^2; m_{t_2}^2)}{2v \sin} \\
&\quad + \frac{3m_t^2 m_t^2 \cos}{32} \frac{\log(m_{t_2}^2 = m_{t_1}^2)}{2v \tan (m_{t_2}^2 - m_{t_1}^2)} ;
\end{aligned}$$

$$\begin{aligned}
M_{15}^t &= \frac{3m_t^2 A_t \sin t}{8} \frac{m_t^2 x}{2v \tan} + \frac{\cos t}{2} \frac{g(m_{t_1}^2; m_{t_2}^2)}{(m_{t_2}^2 - m_{t_1}^2)^2} \\
&\quad + \frac{3m_t^2 m_t^2 A_t \cos}{32} \frac{\log(m_{t_2}^2 = m_{t_1}^2)}{2v \tan (m_{t_2}^2 - m_{t_1}^2)} ;
\end{aligned}$$

$$\begin{aligned}
M_{23}^t &= \frac{3m_t^2 A_t x \sin t}{8^2 v^2 \sin^2} \frac{m_t^2 A_t t_2}{\sin} \frac{\sin t}{2} \frac{g(m_{t_1}^2; m_{t_2}^2)}{(m_{t_2}^2 - m_{t_1}^2)^2} \\
&\quad + \frac{3m_t^2 x A_t \sin t}{16^2 v^2 \sin} \frac{2m_t^2}{\sin^2} \frac{m_Z^2}{2} \frac{\log(m_{t_2}^2 - m_{t_1}^2)}{(m_{t_2}^2 - m_{t_1}^2)}; \\
M_{24}^t &= \frac{3m_t^2 t_1}{8^2 v \tan} \frac{m_t^2 A_t t_2}{\sin} \frac{\sin t}{2} \frac{g(m_{t_1}^2; m_{t_2}^2)}{(m_{t_2}^2 - m_{t_1}^2)^2} \\
&\quad + \frac{3m_t^2 \cos t_1}{16^2 v} \frac{2m_t^2}{\sin^2} \frac{m_Z^2}{2} \frac{\log(m_{t_2}^2 - m_{t_1}^2)}{(m_{t_2}^2 - m_{t_1}^2)}; \\
M_{25}^t &= \frac{3m_t^2 A_t \sin t}{8^2 v \tan} \frac{m_t^2 A_t t_2}{\sin} \frac{\sin t}{2} \frac{g(m_{t_1}^2; m_{t_2}^2)}{(m_{t_2}^2 - m_{t_1}^2)^2} \\
&\quad + \frac{3m_t^2 A_t \sin t}{16^2 v \sin \tan} \frac{2m_t^2}{\sin^2} \frac{m_Z^2 \sin^2}{2} \frac{\log(m_{t_2}^2 - m_{t_1}^2)}{(m_{t_2}^2 - m_{t_1}^2)}; \\
M_{34}^t &= \frac{3m_t^4 x A_t \sin t}{8^2 v \sin^2 \tan} \frac{g(m_{t_1}^2; m_{t_2}^2)}{(m_{t_2}^2 - m_{t_1}^2)^2}; \\
M_{35}^t &= \frac{3m_t^4 x A_t^2 \sin^2 t}{8^2 v \sin^2 \tan} \frac{g(m_{t_1}^2; m_{t_2}^2)}{(m_{t_2}^2 - m_{t_1}^2)^2}; \\
M_{45}^t &= \frac{3m_t^4 A_t \sin t}{8^2 \tan^2} \frac{g(m_{t_1}^2; m_{t_2}^2)}{(m_{t_2}^2 - m_{t_1}^2)^2}; \tag{32}
\end{aligned}$$

where

$$\begin{aligned}
t_1 &= A_t \cos t + x \cot t; \\
t_2 &= A_t + x \cot t \cos t; \\
t &= \frac{4m_W^2}{3} \frac{5m_Z^2}{6} (m_Q^2 - m_T^2) + \frac{4m_W^2}{3} \frac{5m_Z^2}{6} \cos 2t; \tag{33}
\end{aligned}$$

$$g(m_1^2; m_2^2) = \frac{m_2^2 + m_1^2}{m_1^2 - m_2^2} \log \frac{m_2^2}{m_1^2} + 2;$$

Appendix C

The elements for the mass matrix of the neutral Higgs bosons due to the radiative contributions of the bottom quark and scalar bottom quarks are

$$\begin{aligned}
M_{11}^b &= \frac{3}{8^2 v^2} \frac{m_b^2 A_b \cos B_1}{\cos B} + \frac{\cos B}{2} \frac{g(m_{B_1}^2; m_{B_2}^2)}{(m_{B_2}^2 - m_{B_1}^2)^2} \frac{3m_b^4}{4^2 v^2 \cos^2} \log \frac{m_b^2}{2} \\
&\quad + \frac{3 \cos^2}{16^2 v^2} \frac{m_Z^2}{6} \frac{2m_W^2}{3} f(m_{B_1}^2; m_{B_2}^2) \\
&\quad + \frac{3 \cos}{16^2 v^2} \frac{4m_b^2}{\cos^2} \frac{m_Z^2}{2} \frac{m_b^2 A_b \cos B_1}{\cos B} + \frac{\cos B}{2} \frac{\log(m_{B_2}^2 - m_{B_1}^2)}{(m_{B_2}^2 - m_{B_1}^2)} \\
&\quad + \frac{3}{32^2 v^2} \frac{2m_b^2}{\cos} \frac{m_Z^2 \cos}{2} \log \left(\frac{m_{B_1}^2 m_{B_2}^2}{4} A \right);
\end{aligned}$$

$$M_{22}^b = \frac{3}{8} \frac{\left(\frac{m_b^2 x_{b_2}}{\cos \frac{b_2}{2}} \frac{\sin \frac{b_2}{2}}{2} \right)^2}{2v^2} \frac{g(m_{b_1}^2; m_{b_2}^2)}{(m_{b_2}^2 m_{b_1}^2)^2} + \frac{3m_z^4 \sin^2}{128} \frac{\log e^{\frac{m_{b_1}^2 m_{b_2}^2}{4}}}{2v^2}$$

$$+ \frac{3 \sin^2}{16} \frac{m_z^2}{2v^2} \frac{2m_w^2}{3} f(m_{b_1}^2; m_{b_2}^2)$$

$$+ \frac{3m_z^2 \sin}{16} \frac{\left(\frac{m_b^2 x_{b_2}}{\cos \frac{b_2}{2}} \frac{\sin \frac{b_2}{2}}{2} \right)}{2v^2} \frac{\log(m_{b_2}^2 = m_{b_1}^2)}{(m_{b_2}^2 m_{b_1}^2)} ;$$

$$M_{33}^b = \frac{3m_b^4 2x_b^2 A_b^2 \sin^2 b}{8} \frac{g(m_{b_1}^2; m_{b_2}^2)}{2v^2 \cos^4} \frac{g(m_{b_1}^2; m_{b_2}^2)}{(m_{b_2}^2 m_{b_1}^2)^2} ;$$

$$M_{44}^b = \frac{3m_b^4 2^2 \frac{b_2}{2} g(m_{b_1}^2; m_{b_2}^2)}{8} \frac{g(m_{b_1}^2; m_{b_2}^2)}{2 \cot^2} \frac{g(m_{b_1}^2; m_{b_2}^2)}{(m_{b_2}^2 m_{b_1}^2)^2} ;$$

$$M_{55}^b = \frac{3m_b^4 2^2 A_b^2 \sin^2 b}{8} \frac{g(m_{b_1}^2; m_{b_2}^2)}{2 \cot^2} \frac{g(m_{b_1}^2; m_{b_2}^2)}{(m_{b_2}^2 m_{b_1}^2)^2} ;$$

$$M_{12}^b = \frac{3}{8} \frac{\left(\frac{m_b^2 x_{b_2}}{\cos \frac{b_2}{2}} \frac{\sin \frac{b_2}{2}}{2} \right)}{2v^2} \frac{\left(\frac{m_b^2 A_b}{\cos \frac{b_2}{2}} + \frac{\cos \frac{b_2}{2}}{2} \right)}{2} \frac{g(m_{b_1}^2; m_{b_2}^2)}{(m_{b_2}^2 m_{b_1}^2)^2}$$

$$+ \frac{3 \sin 2}{32} \frac{m_z^2}{2v^2} \frac{2m_w^2}{3} f(m_{b_1}^2; m_{b_2}^2)$$

$$+ \frac{3 \cos}{32} \frac{4m_b^2}{2v^2} \frac{m_z^2}{\cos^2} \frac{\left(\frac{m_b^2 x_{b_2}}{\cos \frac{b_2}{2}} \frac{\sin \frac{b_2}{2}}{2} \right)}{2} \frac{\log(m_{b_2}^2 = m_{b_1}^2)}{(m_{b_2}^2 m_{b_1}^2)}$$

$$+ \frac{3m_z^2 \sin 2}{64} \frac{\left(\frac{m_b^2 A_b}{\cos^2} + \frac{\cos \frac{b_2}{2}}{2} \right)}{2v^2} \frac{\log(m_{b_2}^2 = m_{b_1}^2)}{(m_{b_2}^2 m_{b_1}^2)}$$

$$+ \frac{3m_z^2 \sin 2}{256} \frac{4m_b^2}{2v^2} \frac{m_z^2}{\cos^2} \log e^{\frac{m_{b_1}^2 m_{b_2}^2}{4}} ;$$

$$M_{13}^b = \frac{3m_b^2 x_{A_b} \sin b}{8} \frac{\left(\frac{m_b^2 A_b}{\cos \frac{b_2}{2}} + \frac{\cos \frac{b_2}{2}}{2} \right)}{2v^2 \cos^2} \frac{g(m_{b_1}^2; m_{b_2}^2)}{(m_{b_2}^2 m_{b_1}^2)^2}$$

$$+ \frac{3m_b^2 x_{A_b} \sin b}{16} \frac{2m_b^2}{2v^2 \cos} \frac{m_z^2}{\cos^2} \frac{\log(m_{b_2}^2 = m_{b_1}^2)}{(m_{b_2}^2 m_{b_1}^2)} ;$$

$$M_{14}^b = \frac{3m_b^2 \frac{b_2}{2}}{8} \frac{\left(\frac{m_b^2 A_b}{\cos \frac{b_2}{2}} + \frac{\cos \frac{b_2}{2}}{2} \right)}{2v \cot} \frac{g(m_{b_1}^2; m_{b_2}^2)}{(m_{b_2}^2 m_{b_1}^2)^2}$$

$$+ \frac{3m_b^2 \cos \frac{b_2}{2}}{32} \frac{4m_b^2}{2v \cot} \frac{m_z^2}{\cos^2} \frac{\log(m_{b_2}^2 = m_{b_1}^2)}{(m_{b_2}^2 m_{b_1}^2)} ;$$

$$M_{15}^b = \frac{3m_b^2 A_b \sin b}{8} \frac{m_b^2 A_b}{2v \cot} \frac{\left(\frac{m_b^2 A_b}{\cos \frac{b_2}{2}} + \frac{\cos \frac{b_2}{2}}{2} \right)}{2} \frac{g(m_{b_1}^2; m_{b_2}^2)}{(m_{b_2}^2 m_{b_1}^2)^2}$$

$$+ \frac{3m_b^2 A_b \cos \sin b}{32} \frac{4m_b^2}{2v \cot} \frac{m_z^2}{\cos^2} \frac{\log(m_{b_2}^2 = m_{b_1}^2)}{(m_{b_2}^2 m_{b_1}^2)} ;$$

$$\begin{aligned}
M_{23}^b &= \frac{3m_b^2 x A_b \sin_b}{8^2 v^2 \cos^2} \frac{m_b^2 x_{B_2}}{\cos} \frac{\sin_b}{2} \frac{g(m_{B_1}^2; m_{B_2}^2)}{(m_{B_2}^2 - m_{B_1}^2)^2} \\
&\quad + \frac{3m_Z^2 m_b^2 x A_b \tan_b \sin_b \log(m_{B_2}^2 - m_{B_1}^2)}{32^2 v^2 \cos} \frac{g(m_{B_1}^2; m_{B_2}^2)}{(m_{B_2}^2 - m_{B_1}^2)^2}; \\
M_{24}^b &= \frac{3m_b^2 m_{B_2}}{8^2 v \cot} \frac{m_b^2 x_{B_2}}{\cos} \frac{\sin_b}{2} \frac{g(m_{B_1}^2; m_{B_2}^2)}{(m_{B_2}^2 - m_{B_1}^2)^2} \frac{3m_b^2 x \tan_b}{8^2 v \cos} f(m_{B_1}^2; m_{B_2}^2) \\
&\quad + \frac{3m_Z^2 m_b^2 \sin_b \log(m_{B_2}^2 - m_{B_1}^2)}{32^2 v \cot} \frac{g(m_{B_1}^2; m_{B_2}^2)}{(m_{B_2}^2 - m_{B_1}^2)^2}; \\
M_{25}^b &= \frac{3m_b^2 A_b \sin_b}{8^2 v \cot} \frac{m_b^2 x_{B_2}}{\cos} \frac{\sin_b}{2} \frac{g(m_{B_1}^2; m_{B_2}^2)}{(m_{B_2}^2 - m_{B_1}^2)^2} \\
&\quad + \frac{3m_Z^2 m_b^2 A_b \sin_b \log(m_{B_2}^2 - m_{B_1}^2)}{32^2 v \cot} \frac{g(m_{B_1}^2; m_{B_2}^2)}{(m_{B_2}^2 - m_{B_1}^2)^2}; \\
M_{34}^b &= \frac{3m_b^4 x A_b \sin_b}{8^2 v \cos^2 \cot} \frac{g(m_{B_1}^2; m_{B_2}^2)}{(m_{B_2}^2 - m_{B_1}^2)^2}; \\
M_{35}^b &= \frac{3m_b^4 x A_b^2 \sin_b^2}{8^2 v \cos^2 \cot} \frac{g(m_{B_1}^2; m_{B_2}^2)}{(m_{B_2}^2 - m_{B_1}^2)^2}; \\
M_{45}^b &= \frac{3m_b^4 A_b \sin_b}{8^2 \cot^2} \frac{g(m_{B_1}^2; m_{B_2}^2)}{(m_{B_2}^2 - m_{B_1}^2)^2}; \tag{34}
\end{aligned}$$

where

$$\begin{aligned}
B_1 &= A_b + x \tan_b \cos_b; \\
B_2 &= A_b \cos_b + x \tan_b; \\
B &= \frac{m_Z^2}{6} \frac{2m_W^2}{3} m_Q^2 m_B^2 + \frac{m_Z^2}{6} \frac{2m_W^2}{3} \cos 2\beta; \tag{35}
\end{aligned}$$

Appendix D

The elements for the mass matrix of the neutral Higgs bosons due to the radiative contributions of the tau lepton and scalar tau leptons are

$$\begin{aligned}
M_{11} &= \frac{1}{8^2 v^2} \left(\frac{m^2 A_{\tau_1}}{\cos} + \frac{\cos}{2} \right)^2 \frac{g(m_{\tau_1}^2; m_{\tau_2}^2)}{(m_{\tau_2}^2 - m_{\tau_1}^2)^2} \frac{m^4}{4^2 v^2 \cos^2} \log \frac{m_{\tau_2}^2}{m_{\tau_1}^2} \\
&\quad + \frac{\cos^2}{16^2 v^2} \frac{3m_Z^2}{4} m_W^2 f(m_{\tau_1}^2; m_{\tau_2}^2) \\
&\quad + \frac{\cos}{16^2 v^2} \frac{4m^2}{\cos^2} m_Z^2 \left(\frac{m^2 A_{\tau_1}}{\cos} + \frac{\cos}{2} \right) \frac{\log(m_{\tau_2}^2 - m_{\tau_1}^2)}{(m_{\tau_2}^2 - m_{\tau_1}^2)^2} \\
&\quad + \frac{1}{32^2 v^2} \frac{2m^2}{\cos} \frac{m_Z^2 \cos}{2} \log \frac{m_{\tau_1}^2 m_{\tau_2}^2}{4}; \\
M_{22} &= \frac{1}{8^2 v^2} \frac{m^2 x_{\tau_2}}{\cos} \frac{\sin_b}{2} \frac{g(m_{\tau_1}^2; m_{\tau_2}^2)}{(m_{\tau_2}^2 - m_{\tau_1}^2)^2} + \frac{m_Z^4 \sin^2}{128^2 v^2} \log \frac{m_{\tau_1}^2 m_{\tau_2}^2}{4};
\end{aligned}$$

$$\begin{aligned}
& \frac{\sin^2}{16^2 v^2} \frac{3m_z^2}{4} m_w^2 f(m_{\tau_1}^2; m_{\tau_2}^2) \\
& + \frac{m_z^2 \sin}{16^2 v^2} \frac{m^2 x_{\tau_2} \sin}{\cos} \frac{\log(m_{\tau_2}^2 = m_{\tau_1}^2)}{(m_{\tau_2}^2 m_{\tau_1}^2)} ; \\
M_{33} &= \frac{m^4 x^2 A^2 \sin^2}{8^2 v^2 \cos^4} \frac{g(m_{\tau_1}^2; m_{\tau_2}^2)}{(m_{\tau_2}^2 m_{\tau_1}^2)^2} ; \\
M_{44} &= \frac{m^4 x^2 g(m_{\tau_1}^2; m_{\tau_2}^2)}{8^2 \cot^2} \frac{g(m_{\tau_1}^2; m_{\tau_2}^2)}{(m_{\tau_2}^2 m_{\tau_1}^2)^2} ; \\
M_{55} &= \frac{m^4 x^2 A^2 \sin^2}{8^2 \cot^2} \frac{g(m_{\tau_1}^2; m_{\tau_2}^2)}{(m_{\tau_2}^2 m_{\tau_1}^2)^2} ; \\
M_{12} &= \frac{1}{8^2 v^2} \frac{m^2 x_{\tau_2} \sin}{\cos} \frac{m^2 A}{\cos} + \frac{\cos}{2} \frac{g(m_{\tau_1}^2; m_{\tau_2}^2)}{(m_{\tau_2}^2 m_{\tau_1}^2)^2} \\
& + \frac{\sin 2}{32^2 v^2} \frac{3m_z^2}{4} m_w^2 f(m_{\tau_1}^2; m_{\tau_2}^2) \\
& + \frac{\cos}{32^2 v^2} \frac{4m^2}{\cos^2} m_z^2 \frac{m^2 x_{\tau_2} \sin}{\cos} \frac{\log(m_{\tau_2}^2 = m_{\tau_1}^2)}{(m_{\tau_2}^2 m_{\tau_1}^2)} \\
& + \frac{m_z^2 \sin 2}{64^2 v^2} \frac{m^2 A}{\cos^2} + \frac{\log(m_{\tau_2}^2 = m_{\tau_1}^2)}{2(m_{\tau_2}^2 m_{\tau_1}^2)} \\
& + \frac{m_z^2 \sin 2}{256^2 v^2} \frac{4m^2}{\cos^2} m_z^2 \log \frac{m_{\tau_1}^2 m_{\tau_2}^2}{4} ; \\
M_{13} &= \frac{m^2 x A \sin}{8^2 v^2 \cos^2} \frac{m^2 A}{\cos} + \frac{\cos}{2} \frac{g(m_{\tau_1}^2; m_{\tau_2}^2)}{(m_{\tau_2}^2 m_{\tau_1}^2)^2} \\
& \frac{m^2 x A \sin}{16^2 v^2 \cos} \frac{2m^2}{\cos^2} \frac{m_z^2}{2} \frac{\log(m_{\tau_2}^2 = m_{\tau_1}^2)}{(m_{\tau_2}^2 m_{\tau_1}^2)} ; \\
M_{14} &= \frac{m^2}{8^2 v \cot} \frac{m^2 A}{\cos} + \frac{\cos}{2} \frac{g(m_{\tau_1}^2; m_{\tau_2}^2)}{(m_{\tau_2}^2 m_{\tau_1}^2)^2} \\
& + \frac{m^2 \cos}{32^2 v \cot} \frac{4m^2}{\cos^2} m_z^2 \frac{\log(m_{\tau_2}^2 = m_{\tau_1}^2)}{(m_{\tau_2}^2 m_{\tau_1}^2)} ; \\
M_{15} &= \frac{m^2 A \sin}{8^2 v \cot} \frac{m^2 A}{\cos} + \frac{\cos}{2} \frac{g(m_{\tau_1}^2; m_{\tau_2}^2)}{(m_{\tau_2}^2 m_{\tau_1}^2)^2} \\
& \frac{m^2 A \cos \sin}{32^2 v \cot} \frac{4m^2}{\cos^2} m_z^2 \frac{\log(m_{\tau_2}^2 = m_{\tau_1}^2)}{(m_{\tau_2}^2 m_{\tau_1}^2)} ; \\
M_{23} &= \frac{m^2 x A \sin}{8^2 v^2 \cos^2} \frac{m^2 x_{\tau_2} \sin}{\cos} \frac{\log(m_{\tau_2}^2 = m_{\tau_1}^2)}{2(m_{\tau_2}^2 m_{\tau_1}^2)^2} \\
& \frac{m_z^2 m^2 x A \tan \sin}{32^2 v^2 \cos} \frac{\log(m_{\tau_2}^2 = m_{\tau_1}^2)}{(m_{\tau_2}^2 m_{\tau_1}^2)} ; \\
M_{24} &= \frac{m^2}{8^2 v \cot} \frac{m^2 x_{\tau_2} \sin}{\cos} \frac{\log(m_{\tau_2}^2 = m_{\tau_1}^2)}{2(m_{\tau_2}^2 m_{\tau_1}^2)^2} \frac{m^2 x \tan}{8^2 v \cos} f(m_{\tau_1}^2; m_{\tau_2}^2)
\end{aligned}$$

$$\begin{aligned}
& + \frac{m_Z^2 m^2 \sin^2 \alpha}{32 v^2 \cot^2 \alpha} \frac{\log(m_{\tilde{2}}^2 - m_{\tilde{1}}^2)}{(m_{\tilde{2}}^2 - m_{\tilde{1}}^2)} ; \\
M_{25} & = \frac{m^2 A \sin^2 \alpha}{8 v^2 \cot^2 \alpha} \frac{m^2 x \sin^2 \alpha}{\cos^2 \alpha} \frac{g(m_{\tilde{1}}^2; m_{\tilde{2}}^2)}{(m_{\tilde{2}}^2 - m_{\tilde{1}}^2)^2} ; \\
& \frac{m^2 m_Z^2 A \sin^2 \alpha \log(m_{\tilde{2}}^2 - m_{\tilde{1}}^2)}{32 v^2 \cot^2 \alpha (m_{\tilde{2}}^2 - m_{\tilde{1}}^2)} ; \\
M_{34} & = \frac{m^4 x A \sin^2 \alpha}{8 v^2 \cos^2 \alpha \cot^2 \alpha} \frac{g(m_{\tilde{1}}^2; m_{\tilde{2}}^2)}{(m_{\tilde{2}}^2 - m_{\tilde{1}}^2)^2} ; \\
M_{35} & = \frac{m^4 x A^2 \sin^2 \alpha}{8 v^2 \cos^2 \alpha \cot^2 \alpha} \frac{g(m_{\tilde{1}}^2; m_{\tilde{2}}^2)}{(m_{\tilde{2}}^2 - m_{\tilde{1}}^2)^2} ; \\
M_{45} & = \frac{m^4 x A \sin^2 \alpha}{8 v^2 \cot^2 \alpha} \frac{g(m_{\tilde{1}}^2; m_{\tilde{2}}^2)}{(m_{\tilde{2}}^2 - m_{\tilde{1}}^2)^2} ; \tag{36}
\end{aligned}$$

where

$$\begin{aligned}
\tilde{m}_1 & = A + x \tan^2 \alpha ; \\
\tilde{m}_2 & = A \cos^2 \alpha + x \tan^2 \alpha ; \\
\tilde{m} & = \frac{3m_Z^2}{4} m_W^2 m_L^2 m_E^2 + \frac{3m_Z^2}{4} m_W^2 \cos^2 \alpha ; \tag{37}
\end{aligned}$$

Appendix E

The elements for the mass matrix of the neutral Higgs bosons due to the radiative contributions of the W boson, charged Higgs boson, and charginos are

$$\begin{aligned}
M_{11} & = \frac{m_W^4 \cos^2 \alpha}{4 v^2} \frac{g(m_{\tilde{1}}^2; m_{\tilde{2}}^2)}{(m_{\tilde{2}}^2 - m_{\tilde{1}}^2)^2} + \frac{m_W^4 \cos^2 \alpha}{2 v^2} f(m_{\tilde{1}}^2; m_{\tilde{2}}^2) \\
& \frac{m_W^4 \cos^2 \alpha}{2 v^2} \frac{\log(m_{\tilde{2}}^2 - m_{\tilde{1}}^2)}{(m_{\tilde{2}}^2 - m_{\tilde{1}}^2)} + \frac{m_W^4 \cos^2 \alpha}{8 v^2} \log \frac{m_W^6 m_{C^+}^2}{m_{\tilde{1}}^4 m_{\tilde{2}}^4} ; \\
& + \frac{\sin^2 \alpha}{16 v^2} (2 v^2 m_W^2) m_{C^+}^2 \log \frac{m_{C^+}^2}{2} 1 ; \\
M_{22} & = \frac{m_W^4 \sin^2 \alpha}{4 v^2} \frac{g(m_{\tilde{1}}^2; m_{\tilde{2}}^2)}{(m_{\tilde{2}}^2 - m_{\tilde{1}}^2)^2} + \frac{m_W^4 \sin^2 \alpha}{2 v^2} f(m_{\tilde{1}}^2; m_{\tilde{2}}^2) \\
& \frac{m_W^4 \sin^2 \alpha}{2 v^2} \frac{\log(m_{\tilde{2}}^2 - m_{\tilde{1}}^2)}{(m_{\tilde{2}}^2 - m_{\tilde{1}}^2)} + \frac{m_W^4 \sin^2 \alpha}{8 v^2} \log \frac{m_W^6 m_{C^+}^2}{m_{\tilde{1}}^4 m_{\tilde{2}}^4} ; \\
& + \frac{\cos^2 \alpha}{16 v^2} (2 v^2 m_W^2) m_{C^+}^2 \log \frac{m_{C^+}^2}{2} 1 ; \\
M_{33} & = \frac{m_W^4 M_Z^2 x^2 \sin^2 \alpha}{2 v^2 (m_{\tilde{2}}^2 - m_{\tilde{1}}^2)^2} g(m_{\tilde{1}}^2; m_{\tilde{2}}^2) \\
& \frac{(2 v^2 m_W^2) m_{C^+}^2}{16 v^2} \log \frac{m_{C^+}^2}{2} 1 ; \\
M_{44} & = \frac{2 v^2 g(m_{\tilde{1}}^2; m_{\tilde{2}}^2)}{16 v^2 (m_{\tilde{2}}^2 - m_{\tilde{1}}^2)^2} + \frac{4 x^2}{8 v^2} f(m_{\tilde{1}}^2; m_{\tilde{2}}^2) \frac{4 x^2}{16 v^2} \log \frac{m_{\tilde{1}}^2 m_{\tilde{2}}^2}{4} ;
\end{aligned}$$

$$\begin{aligned}
& \frac{3x}{8^2} \frac{\sim \log(m_{\sim 2}^2 = m_{\sim 1}^2)}{(m_{\sim 2}^2 m_{\sim 1}^2)} \frac{A \sin 2 m_{C^+}^2}{32^2 x} \log \frac{m_{C^+}^2}{2} 1 ; \\
M_{55} = & \frac{m_W^4 M_2^2 \sin^2 2 \sin^2 c}{4^2 (m_{\sim 2}^2 m_{\sim 1}^2)^2} g(m_{\sim 1}^2; m_{\sim 2}^2) \\
& \frac{\sin 2}{32^2 x} (A + 8kx) m_{C^+}^2 \log \frac{m_{C^+}^2}{2} 1 ; \\
M_{12} = & \frac{m_W^4 \sin 2}{8^2 v^2} \frac{\sim_1 \sim_2}{(m_{\sim 2}^2 m_{\sim 1}^2)^2} g(m_{\sim 1}^2; m_{\sim 2}^2) \frac{m_W^4 \sin 2}{4^2 v^2} f(m_{\sim 1}^2; m_{\sim 2}^2) \\
& \frac{m_W^4 \sin 2}{8^2 v^2} \frac{(\sim_1 + \sim_2)}{(m_{\sim 2}^2 m_{\sim 1}^2)} \log \frac{m_{\sim 2}^2}{m_{\sim 1}^2} + \frac{m_W^4 \sin 2}{16^2 v^2} \log \frac{m_W^6 m_{C^+}^2}{(m_{\sim 1}^4 m_{\sim 2}^4)} \\
& \frac{2m_W^2 \sin 2}{8^2} \log \frac{m_{C^+}^2}{2} + \frac{\sin 2}{32^2 v^2} (m_W^2 2^2 v^2) m_{C^+}^2 \log \frac{m_{C^+}^2}{2} 1 ; \\
M_{13} = & \frac{m_W^4 M_2 x \cos \sin c}{2^2 v^2} \frac{\sim_1}{(m_{\sim 2}^2 m_{\sim 1}^2)^2} g(m_{\sim 1}^2; m_{\sim 2}^2) \\
& \frac{m_W^4 M_2 x \cos \sin c}{2^2 v^2} \frac{\sim_1}{(m_{\sim 2}^2 m_{\sim 1}^2)} \log \frac{m_{\sim 2}^2}{m_{\sim 1}^2} ; \\
M_{14} = & \frac{m_W^2 \cos \sim_1}{8^2 v} \frac{\sim_2}{(m_{\sim 2}^2 m_{\sim 1}^2)^2} g(m_{\sim 1}^2; m_{\sim 2}^2) + \frac{m_W^2 2x \cos}{4^2 v} f(m_{\sim 1}^2; m_{\sim 2}^2) \\
& \frac{m_W^2 2x \cos}{8^2 v} \log \frac{m_{\sim 1}^2 m_{\sim 2}^2}{4} + \frac{m_W^2 \cos (\sim_1 + \sim_2)}{8^2 v} \frac{\sim_1}{(m_{\sim 2}^2 m_{\sim 1}^2)} \log \frac{m_{\sim 2}^2}{m_{\sim 1}^2} ; \\
M_{15} = & \frac{m_W^4 M_2 \cos \sin 2 \sin c}{4^2 v} \frac{\sim_1}{(m_{\sim 2}^2 m_{\sim 1}^2)^2} g(m_{\sim 1}^2; m_{\sim 2}^2) \\
& \frac{m_W^4 M_2 \cos \sin 2 \sin c}{4^2 v} \frac{\sim_1}{(m_{\sim 2}^2 m_{\sim 1}^2)} \log \frac{m_{\sim 2}^2}{m_{\sim 1}^2} ; \\
M_{23} = & \frac{m_W^4 M_2 x \sin \sin c}{2^2 v^2} \frac{\sim_2}{(m_{\sim 2}^2 m_{\sim 1}^2)^2} g(m_{\sim 1}^2; m_{\sim 2}^2) \\
& \frac{m_W^4 M_2 x \sin \sin c}{2^2 v^2} \frac{\sim_2}{(m_{\sim 2}^2 m_{\sim 1}^2)} \log \frac{m_{\sim 2}^2}{m_{\sim 1}^2} ; \\
M_{24} = & \frac{m_W^2 \sin \sim_2}{8^2 v} \frac{\sim_1}{(m_{\sim 2}^2 m_{\sim 1}^2)^2} g(m_{\sim 1}^2; m_{\sim 2}^2) + \frac{m_W^2 2x \sin}{4^2 v} f(m_{\sim 1}^2; m_{\sim 2}^2) \\
& \frac{m_W^2 2x \sin}{8^2 v} \log \frac{m_{\sim 1}^2 m_{\sim 2}^2}{4} + \frac{m_W^2 \sin (\sim_2 + \sim_1)}{8^2 v} \frac{\sim_2}{(m_{\sim 2}^2 m_{\sim 1}^2)} \log \frac{m_{\sim 2}^2}{m_{\sim 1}^2} ; \\
M_{25} = & \frac{m_W^4 M_2 \sin \sin 2 \sin c}{4^2 v} \frac{\sim_2}{(m_{\sim 2}^2 m_{\sim 1}^2)^2} g(m_{\sim 1}^2; m_{\sim 2}^2) \\
& + \frac{m_W^4 M_2 \sin \sin 2 \sin c}{4^2 v} \frac{\sim_2}{(m_{\sim 2}^2 m_{\sim 1}^2)} \log \frac{m_{\sim 2}^2}{m_{\sim 1}^2} ; \\
M_{34} = & \frac{m_W^2 M_2 2x \sin c}{4^2 v} \frac{\sim_1}{(m_{\sim 2}^2 m_{\sim 1}^2)^2} g(m_{\sim 1}^2; m_{\sim 2}^2) \frac{m_W^2 M_2 3x^2 \sin c}{4^2 v} \frac{\sim_2}{(m_{\sim 2}^2 m_{\sim 1}^2)} \log \frac{m_{\sim 2}^2}{m_{\sim 1}^2} ;
\end{aligned}$$

$$\begin{aligned}
M_{35} &= \frac{m_W^4}{2^2 v} \frac{M_2^2 x \sin 2\alpha \sin^2 \beta_c}{(m_{\tilde{2}}^2 - m_{\tilde{1}}^2)^2} g(m_{\tilde{1}}^2; m_{\tilde{2}}^2) + \frac{m_W^2}{2^2 v} M_2 \cos \beta_c f(m_{\tilde{1}}^2; m_{\tilde{2}}^2); \\
M_{45} &= \frac{m_W^2}{8^2} \frac{M_2^2 \sin 2\alpha \sin \beta_c}{(m_{\tilde{2}}^2 - m_{\tilde{1}}^2)^2} g(m_{\tilde{1}}^2; m_{\tilde{2}}^2) \\
&\quad + \frac{m_W^2}{8^2} \frac{M_2^3 x \sin 2\alpha \sin \beta_c}{(m_{\tilde{2}}^2 - m_{\tilde{1}}^2)} \log \frac{m_{\tilde{2}}^2}{m_{\tilde{1}}^2}; \tag{38}
\end{aligned}$$

where

$$\begin{aligned}
\tilde{m}_1 &= M_2^2 + x^2 + 2m_W^2 \cos 2\alpha + 2xM_2 \tan \beta_c \cos \beta_c; \\
\tilde{m}_2 &= M_2^2 + x^2 - 2m_W^2 \cos 2\alpha + 2xM_2 \cot \beta_c \cos \beta_c; \\
\tilde{m} &= x^3 + xM_2^2 + 2xm_W^2 + 2m_W^2 M_2 \sin 2\alpha \cos \beta_c; \tag{39}
\end{aligned}$$

Appendix F

The elements for the field-dependent mass matrix of the scalar Higgs bosons at the tree level are

$$\begin{aligned}
M_{S_{11}} &= \frac{3}{v} m_Z^2 \cos \beta_c h_1 + 2v^2 \frac{m_Z^2}{v} \sin \beta_c h_2 + 2x^2 h_4 + \frac{3m_Z^2 h_1^2}{2v^2} + 2 \frac{m_Z^2}{2v^2} h_2^2 \\
&\quad + \cos^2 \beta_c \frac{m_Z^2 \cos 2\alpha}{2v^2} h_3^2 + h_4^2 + h_5^2 + m_Z^2 \cos^2 \beta_c \\
&\quad + x(A + kx) \tan \beta_c; \\
M_{S_{22}} &= 2v^2 \frac{m_Z^2}{v} \cos \beta_c h_1 + \frac{3}{v} m_Z^2 \sin \beta_c h_2 + 2x^2 h_4 + 2 \frac{m_Z^2}{2v^2} h_1^2 + \frac{3}{2v^2} m_Z^2 h_2^2 \\
&\quad + \sin^2 \beta_c \frac{m_Z^2 \cos 2\alpha}{2v^2} h_3^2 + h_4^2 + h_5^2 + m_Z^2 \sin^2 \beta_c \\
&\quad + x(A + kx) \cot \beta_c; \\
M_{S_{33}} &= 2v(\cos \beta_c - k \sin \beta_c) h_1 + 2v(\sin \beta_c - k \cos \beta_c) h_2 + 2k(6kx - A_k) h_4 + 2h_1^2 \\
&\quad + h_2^2 + (A + k \sin 2\alpha) h_3^2 + 6k^2 h_4^2 + 2k^2 h_5^2 - 2k h_1 h_2 + \frac{v^2}{2x} A \sin 2\alpha \\
&\quad - A_k kx + 4k^2 x^2; \\
M_{S_{12}} &= 2^2 v \frac{m_Z^2}{v} (\sin \beta_c h_1 + \cos \beta_c h_2) - (A + 2kx) h_4 - k h_4^2 + k h_5^2 \\
&\quad + 2^2 \frac{m_Z^2}{v^2} h_1 h_2 - x(A + kx) + 2v^2 \frac{m_Z^2}{2} \sin 2\alpha; \\
M_{S_{13}} &= 2x^2 h_1 - (A + 2kx) h_2 + 2v(\cos \beta_c - k \sin \beta_c) h_4 + 2^2 h_1 h_4 - 2k h_2 h_4 \\
&\quad - 2k \cos \beta_c h_3 h_5 + 2vx^2 \cos \beta_c - v(A + 2kx) \sin \beta_c; \\
M_{S_{23}} &= (A + 2kx) h_1 + 2x^2 h_2 + 2v(\sin \beta_c - k \cos \beta_c) h_4 - 2k h_1 h_4 + 2^2 h_2 h_4 \\
&\quad - 2k \sin \beta_c h_3 h_5 + 2vx^2 \sin \beta_c - v(A + 2kx) \cos \beta_c; \tag{40}
\end{aligned}$$

Appendix G

The elements for the field-dependent mass matrix of the pseudoscalar Higgs bosons at the tree level are

$$\begin{aligned}
M_{P_{44}} &= \frac{1}{v} (2\sqrt{v^2 \cos^2 \theta} - m_Z^2 \cos 2\theta) \cos h_1 + \frac{1}{v} (2\sqrt{v^2 \sin^2 \theta} + m_Z^2 \sin 2\theta) \sin h_2 \\
&+ f_2 x (A + 2kx) \sin 2\theta gh_3 + \frac{1}{2v^2} (2\sqrt{v^2 \cos^2 \theta} - m_Z^2 \cos 2\theta) \cos h_1^2 \\
&+ \frac{1}{2v^2} (2\sqrt{v^2 \sin^2 \theta} - m_Z^2 \cos 2\theta) \cos h_2^2 \\
&+ \frac{3}{4v^2} f_2 \sqrt{v^2 \sin^2 \theta} + m_Z^2 (1 + \cos 4\theta) gh_3^2 + (k + k \sin 2\theta) h_4 \\
&+ (k \sin 2\theta) h_5 + \frac{2x(A + kx)}{\sin 2\theta} ; \\
M_{P_{55}} &= 2(v \cos \theta + kv \sin \theta) h_1 + 2(v \sin \theta + kv \cos \theta) h_2 + 2k(A_k + 2kx) h_4 \\
&+ h_1^2 + h_2^2 + (k \sin 2\theta) h_3^2 + 2k^2 h_4^2 + 6k^2 h_5^2 + 2kh_1 h_2 + 3A_k kx \\
&+ v^2 2k + \frac{A}{2x} \sin 2\theta ; \\
M_{P_{45}} &= (A - 2kx) \cos h_1 + (A - 2kx) \sin h_2 - 2k v h_4 - 2k \cos h_1 h_4 \\
&- 2k \sin h_2 h_4 + 2(k \sin 2\theta) h_3 h_5 + v(A - 2kx) ; \tag{41}
\end{aligned}$$

Reference

- [1] A. Pilaftsis, Phys. Lett. B 435, 88 (1998); A. Pilaftsis, Phys. Rev. D 58, 096010 (1998).
- [2] M. B. Rühl and G. L. Kane, Phys. Lett. B 437, 331 (1998); A. Pilaftsis and C. E. M. Wagner, Nucl. Phys. B 553, 3 (1999); D. A. Demir, Phys. Rev. D 60, 055006 (1999); D. A. Demir, Phys. Rev. D 60, 095007 (1999); S. Y. Choi and J. S. Lee, Phys. Rev. D 61, 015003 (1999); M. Carena, J. Ellis, A. Pilaftsis, and C. E. M. Wagner, Nucl. Phys. B 586, 92 (2000); S. Y. Choi, M. Drees, and J. S. Lee, Phys. Lett. B 481, 57 (2000); S. Bae, Phys. Lett. B 489, 171 (2000); G. L. Kane and L. T. Wang, Phys. Lett. B 488, 383 (2000); S. W. Ham, S. K. Oh, E. J. Yoo, and H. K. Lee, J. Phys. G 27, 1 (2001); M. Carena, J. Ellis, A. Pilaftsis, and C. E. M. Wagner, Phys. Lett. B 495, 155 (2000); T. Ibrahim and P. Nath, Phys. Rev. D 63, 035009 (2001); T. Ibrahim, Phys. Rev. D 64, 035009 (2001); S. Heinemeyer, Eur. Phys. J. C 22, 521 (2001); M. Boz and N. K. Pak, Phys. Rev. D 65, 075014 (2002); M. Carena, J. Ellis, A. Pilaftsis, and C. E. M. Wagner, Nucl. Phys. B 625, 345 (2002); E. Christova, H. Eberl, S. Kramerl, and W. Majerotto, Nucl. Phys. B 639, 263 (2002); N. Ghobane, S. Katsanevas, I. Laktineh, J. Rosiek, Nucl. Phys. B 647, 190 (2002); M. Boz, J. Phys. G 28, 2377 (2002); M. Carena, J. Ellis, S. Mrenna, A. Pilaftsis, and C. E. M. Wagner, Phys. Lett. B 659, 145 (2003).
- [3] T. Ibrahim and P. Nath, Phys. Rev. D 66, 015005 (2002).
- [4] S. W. Ham, S. K. Oh, Y. E. Yoo, C. M. Kim, and D. Son, Phys. Rev. D 68, 055003 (2003).
- [5] M. Matsuda and M. Tanimoto, Phys. Rev. D 52, 3100 (1995); N. Haba, Prog. Theor. Phys. 97, 301 (1997).
- [6] S. W. Ham, J. Kim, S. K. Oh, and D. Son, Phys. Rev. D 64, 035007 (2001).
- [7] S. W. Ham, S. K. Oh, and D. Son, Phys. Rev. D 65, 075004 (2002).
- [8] J. Ellis, J. F. Gunion, H. E. Haber, L. Roszkowski, F. Zwirner, Phys. Rev. D 39, 844 (1989); M. Drees, Int. J. Mod. Phys. A 4, 3635 (1989); J. R. Espinosa and M. Quiros, Phys. Lett. B 266, 389 (1991); P. Binétruy and C. A. Savoy, Phys. Lett. B 277, 453 (1992); J. R. Espinosa and M. Quiros, Phys. Lett. B 279, 92 (1992); U. Ellwanger and M. R. de Trautenberg, Z. Phys. C 53, 521 (1992); U. Ellwanger and M. L. Linder, Phys. Lett. B 301, 365 (1993); J. R. Espinosa and M. Quiros, Phys. Lett. B 302, 51 (1993); U. Ellwanger, Phys. Lett. B 303, 271 (1993); U. Ellwanger, M. R. de Trautenberg, and C. A. Savoy, Phys. Lett. B 315, 331 (1993); P. N. Pandita, Phys. Lett. B 318, 338 (1993); P. N. Pandita, Z. Phys. C 59, 575 (1993); J. I. Kamoshita, Y. Okada, and M. Tanaka, Phys. Lett. B 328, 67 (1994); F. Franke, H. Fraas, and A. Bartl, Phys. Lett. B 336, 415 (1994); P. N. Pandita, Z. Phys. C 63, 659 (1994); T. Elliott, S. F. King, and P. L. White, Phys. Rev. D 49, 2435 (1994); U. Ellwanger, M. R. de Trautenberg, and C. A. Savoy, Z. Phys. C 67, 665 (1995); S. F. King and P. L. White, Phys. Rev. D 52, 4183 (1995); S. F. King and P. L. White, Phys. Rev. D 53, 4049 (1996); B. Ananthanarayan and P. N. Pandita, Phys. Lett. B 371, 245 (1996); S. W. Ham, S. K. Oh, and B. R. Kim, J. Phys. G 22, 1575 (1996); A. Stephan, Phys. Lett. B 411, 97 (1997); M. Drees, E. Ma, P. N. Pandita, D. P. Roy, S. K. Vempati, Phys. Lett. B 433, 346 (1998); M. Masip, R. Muñoz-Tapia, and A. Pomarol, Phys. Rev. D 57, R5340 (1998); A. Stephan, Phys. Rev. D 58, 035011 (1998); S. Hesselbach, F. Franke, and H. Fraas, Phys. Lett. B 492, 140 (2000); R. B. Nevzorov and M. A. Trusov, JETP 91, 1079

(2000); C. Panagiotakopoulos and A. Pilaftsis, *Phys. Lett. B* 505 184 (2001); Y. Mambri, G. Moutaka, M. Rausch, and D. Trautenberg, *Nucl. Phys. B* 609, 83 (2001); U. Ellwanger and C. Hugonie, *Eur. Phys. J. C* 25, 297 (2002); D. J. Miller, R. Nevzorov, and P. M. Zerwas, [hep-ph/0304049](https://arxiv.org/abs/hep-ph/0304049).

[9] F. Franke and H. Fraas, *Phys. Lett. B* 353, 234 (1995); S. W. Ham, S. K. Oh, and B. R. Kin, *Phys. Lett. B* 414, 305 (1997).

[10] S. Coleman and E. Weinberg, *Phys. Rev. D* 7, 1888 (1973).

Figure Captions

Fig. 1 (a) : The plot of the (1;3)-, (2;3)-, and (3;4)-elements of the mass matrix of the neutral Higgs bosons, M_{13} (solid curve), M_{23} (dashed curve), and M_{34} (dotted curve), as a function of $\tan \beta$ for $\mu = \nu = \tau = \rho = \sigma = 8 = 5$, $\tan \alpha = 10$, $\kappa = 0.3$, $A = 300 \text{ GeV}$, $A_k = 200 \text{ GeV}$, $x = A_t = A_b = A = 900 \text{ GeV}$, $m_Q = m_L = M_2 = 800 \text{ GeV}$, and $m_T = m_B = m_E = 400 \text{ GeV}$.

Fig. 1 (b) : The plot of the (1;5)-, (2;5), and (4;5)-elements of the mass matrix of the neutral Higgs bosons, M_{15} (solid curve), M_{25} (dashed curve), and M_{45} (dotted curve), as a function of $\tan \beta$ for $\mu = \nu = \tau = \rho = \sigma = 8 = 5$, $\tan \alpha = 10$, $\kappa = 0.3$, $A = 300 \text{ GeV}$, $A_k = 200 \text{ GeV}$, $x = A_t = A_b = A = 900 \text{ GeV}$, $m_Q = m_L = M_2 = 800 \text{ GeV}$, and $m_T = m_B = m_E = 400 \text{ GeV}$.

Fig. 1 (c) : The plot of the O_{13}^2 (solid curve), O_{23}^2 (dashed curve), and O_{34}^2 (dotted curve), as a function of $\tan \beta$ for $\mu = \nu = \tau = \rho = \sigma = 8 = 5$, $\tan \alpha = 10$, $\kappa = 0.3$, $A = 300 \text{ GeV}$, $A_k = 200 \text{ GeV}$, $x = A_t = A_b = A = 900 \text{ GeV}$, $m_Q = m_L = M_2 = 800 \text{ GeV}$, and $m_T = m_B = m_E = 400 \text{ GeV}$.

Fig. 1 (d) : The plot of the O_{15}^2 (solid curve), O_{25}^2 (dashed curve), and O_{45}^2 (dotted curve), as a function of $\tan \beta$ for $\mu = \nu = \tau = \rho = \sigma = 8 = 5$, $\tan \alpha = 10$, $\kappa = 0.3$, $A = 300 \text{ GeV}$, $A_k = 200 \text{ GeV}$, $x = A_t = A_b = A = 900 \text{ GeV}$, $m_Q = m_L = M_2 = 800 \text{ GeV}$, and $m_T = m_B = m_E = 400 \text{ GeV}$.

Fig. 2a : The plot of the lightest neutral Higgs boson mass, as a function of $\tan \beta$ for $\tan \alpha = 2$ (solid curve), $\tan \alpha = 10$ (dashed curve), $\tan \alpha = 25$ (dotted curve), and $\tan \alpha = 40$ (dot-dashed curve). The remaining parameters are the same as Fig. 1.

Fig. 2b : The plot of the lightest neutral Higgs boson mass, as a function of $\tan \beta$ for $\tan \alpha = 2$ (solid curve), $\tan \alpha = 10$ (dashed curve), $\tan \alpha = 25$ (dotted curve), and $\tan \alpha = 40$ (dot-dashed curve) at $\mu = \nu = 5$. The remaining parameters are the same as Fig. 1.

Fig. 3 : The plot of ρ , as a function of $\tan \beta$ for $\mu = \nu = 5$ (solid curve) and $\mu = \nu = 3 = 5$ (dashed curve). The remaining parameters are the same as Fig. 1.

Fig. 4a : The plot of R_{13} against R_1 , under the condition of $(m_{h_{(n+1)}} - m_{h_{(n)}}) > 10 \text{ GeV}$, where $n = 1$ to 4.

Fig. 4b : The plot of R_{23} against R_1 , under the condition of $(m_{h_{(n+1)}} - m_{h_{(n)}}) > 10 \text{ GeV}$, where $n = 1$ to 4.

Fig. 4c : The plot of R_{34} against R_1 , under the condition of $(m_{h_{(n+1)}} - m_{h_{(n)}}) > 10 \text{ GeV}$, where $n = 1$ to 4.

Fig. 4d : The plot of R_{15} against R_1 , under the condition of $(m_{h_{(n+1)}} - m_{h_{(n)}}) > 10 \text{ GeV}$, where $n = 1$ to 4.

Fig. 4e : The plot of R_{25} against R_1 , under the condition of $(m_{h_{(n+1)}} - m_{h_{(n)}}) > 10 \text{ GeV}$, where $n = 1$ to 4.

Fig. 4f : The plot of R_{45} against R_1 , under the condition of $(m_{h_{(n+1)}} - m_{h_{(n)}}) > 10 \text{ GeV}$, where $n = 1$ to 4.

Fig. 5 : The plot of R_{h1} against R_1 , under the condition of $(m_{h_{(n+1)}} - m_{h_{(n)}}) > 10 \text{ GeV}$, where $n = 1$ to 4.

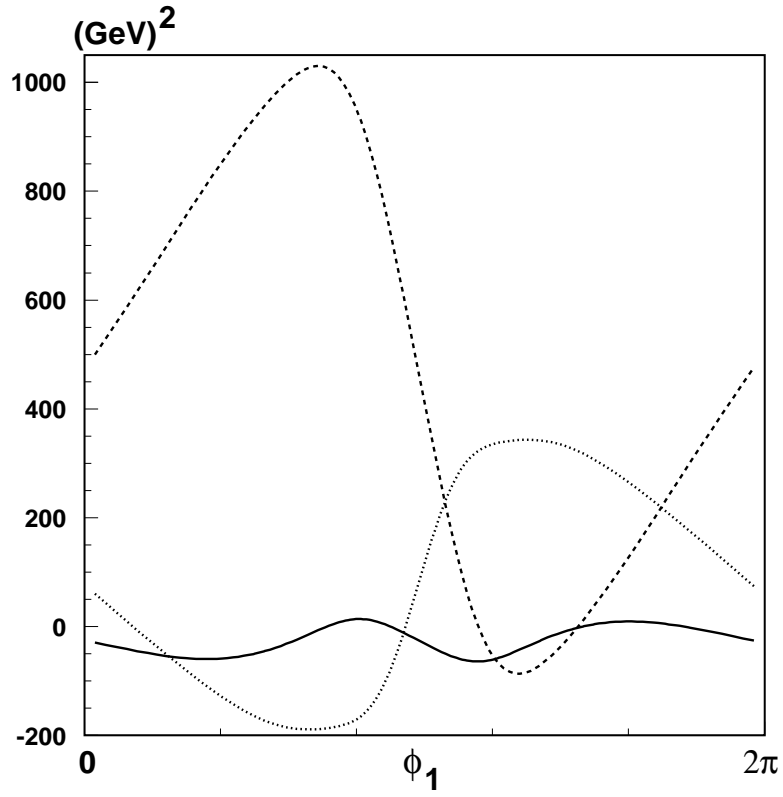


Fig. 1a: The plot of the (1;3)-, (2;3)-, and (3;4)-elements of the mass matrix of the neutral Higgs bosons, M_{13} (solid curve), M_{23} (dashed curve), and M_{34} (dotted curve), as a function of ϕ_1 for $\mu_t = \mu_b = \mu_c = 8 = 5$, $\tan \beta = 10$, $\mu = k = 0.3$, $A = 300 \text{ GeV}$, $A_k = 200 \text{ GeV}$, $\mu_x = A_t = A_b = A = 900 \text{ GeV}$, $m_Q = m_L = M_2 = 800 \text{ GeV}$, and $m_T = m_B = m_E = 400 \text{ GeV}$.

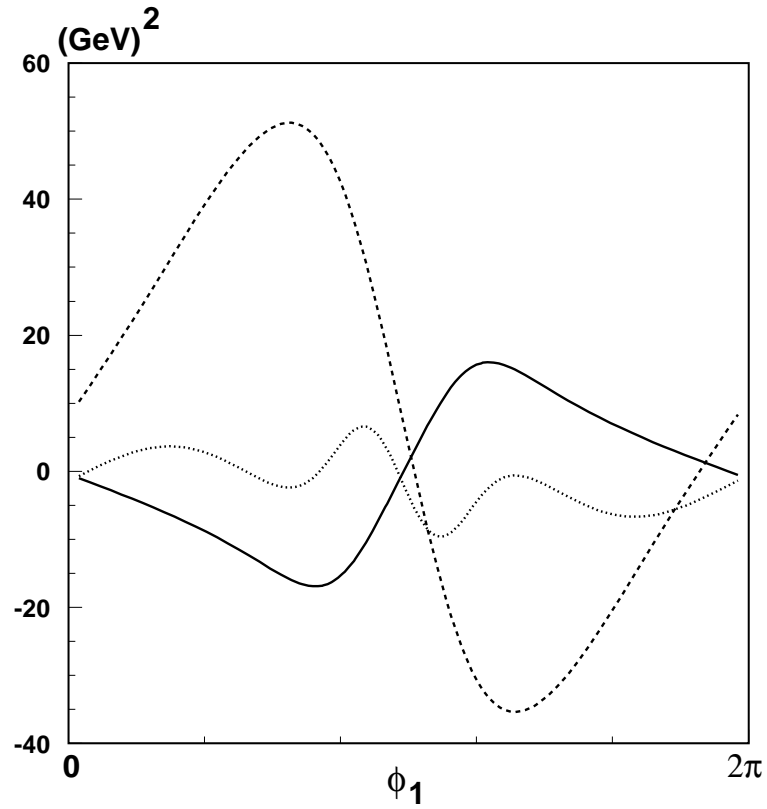


Fig. 1b: The plot of the (1;5), (2;5), and (4;5)-elements of the mass matrix of the neutral Higgs bosons, M_{15} (solid curve), M_{25} (dashed curve), and M_{45} (dotted curve), as a function of ϕ_1 for $\mu_t = \mu_b = \mu_c = 8 = 5$, $\tan \beta = 10$, $\mu = k = 0.3$, $A = 300 \text{ GeV}$, $A_k = 200 \text{ GeV}$, $\mu_x = A_t = A_b = A = 900 \text{ GeV}$, $m_Q = m_L = M_2 = 800 \text{ GeV}$, and $m_T = m_B = m_E = 400 \text{ GeV}$.

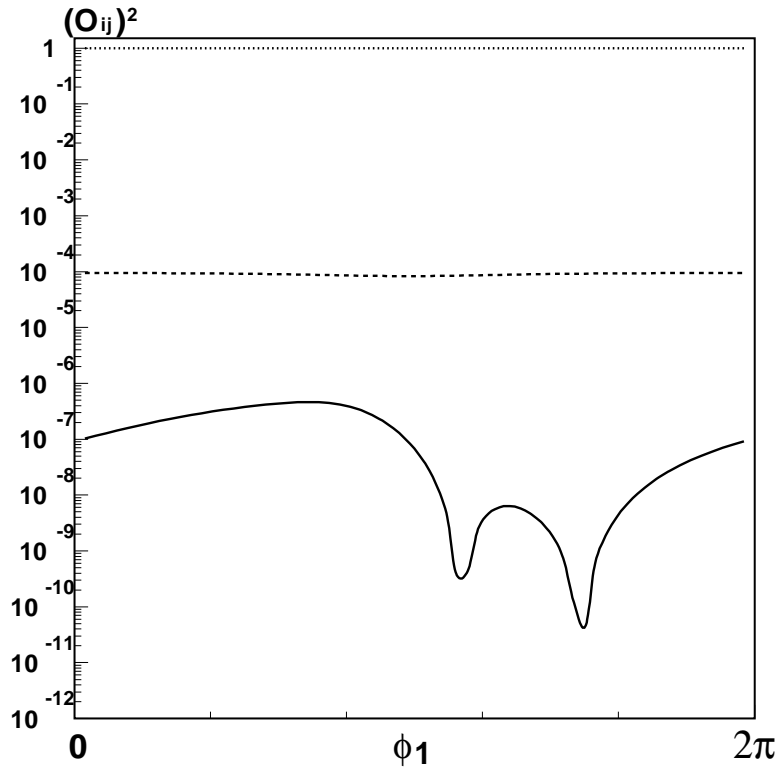


Fig. 1c: The plot of the O_{13}^2 (solid curve), O_{23}^2 (dashed curve), and O_{34}^2 (dotted curve), as a function of ϕ_1 for $t = b = c = 8 = 5$, $\tan \beta = 10$, $k = 0.3$, $A = 300 \text{ GeV}$, $A_k = 200 \text{ GeV}$, $x = A_t = A_b = A = 900 \text{ GeV}$, $m_Q = m_L = M_2 = 800 \text{ GeV}$, and $m_T = m_B = m_E = 400 \text{ GeV}$.

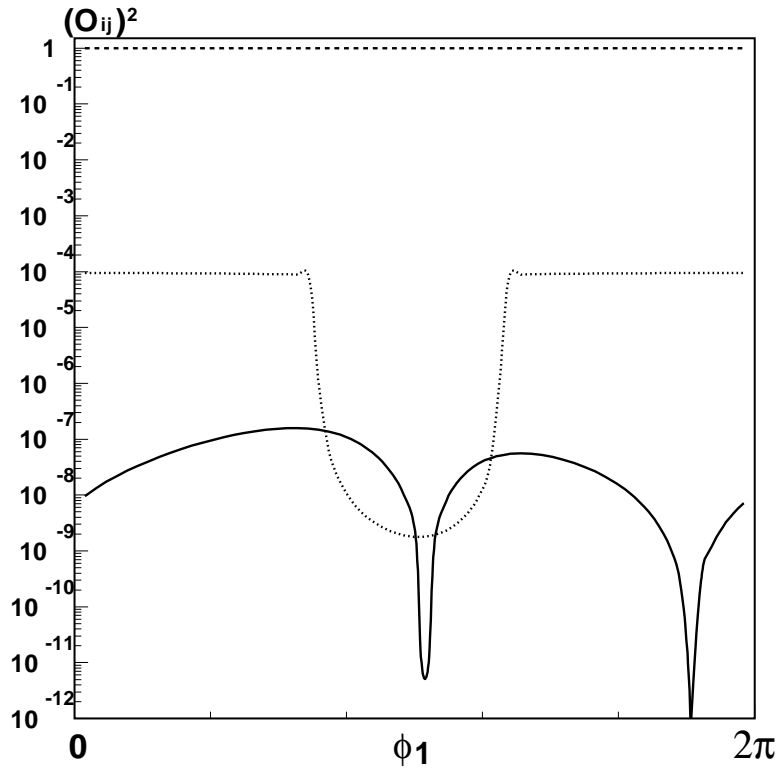


Fig. 1d: The plot of the O_{15}^2 (solid curve), O_{25}^2 (dashed curve), and O_{45}^2 (dotted curve), as a function of ϕ_1 for $t = b = c = 8 = 5$, $\tan \beta = 10$, $k = 0.3$, $A = 300 \text{ GeV}$, $A_k = 200 \text{ GeV}$, $x = A_t = A_b = A_c = 900 \text{ GeV}$, $m_Q = m_L = M_2 = 800 \text{ GeV}$, and $m_T = m_B = m_E = 400 \text{ GeV}$.

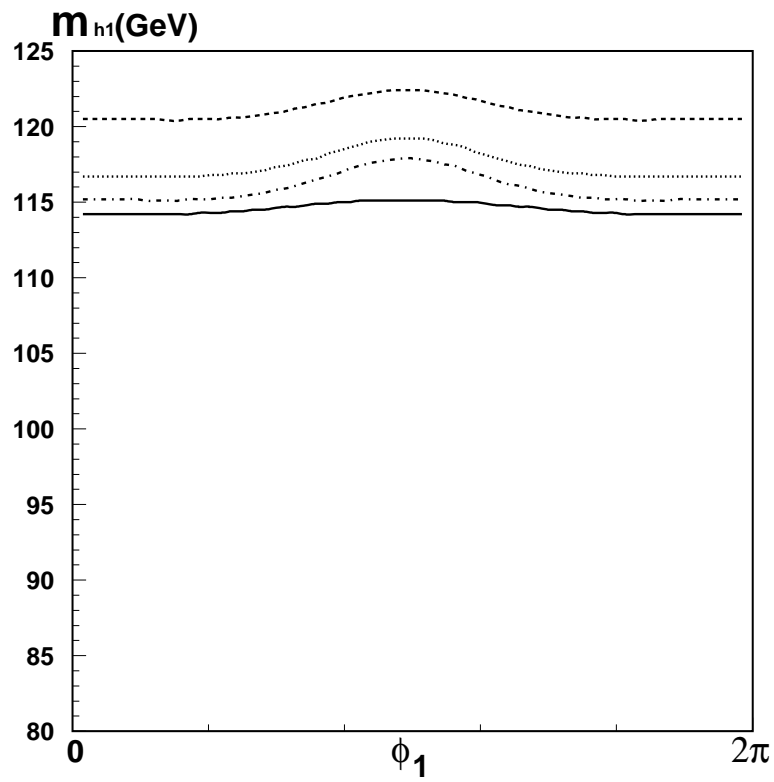


Fig. 2a: The plot of the lightest neutral Higgs boson mass, as a function of ϕ_1 for $\tan\beta = 2$ (solid curve), $\tan\beta = 10$ (dashed curve), $\tan\beta = 25$ (dotted curve), and $\tan\beta = 40$ (dot-dashed curve). The remaining parameters are the same as Fig. 1.

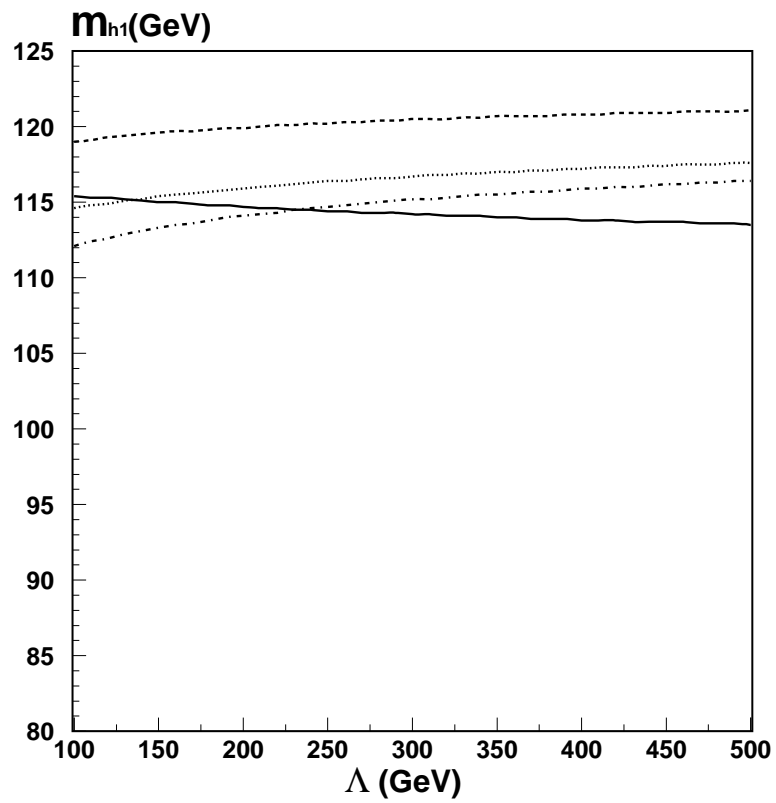


Fig. 2b: The plot of the lightest neutral Higgs boson mass, as a function of Λ for $\tan\beta = 2$ (solid curve), $\tan\beta = 10$ (dashed curve), $\tan\beta = 25$ (dotted curve), and $\tan\beta = 40$ (dot-dashed curve) at $\mu_1 = 5$. The remaining parameters are the same as Fig. 1.

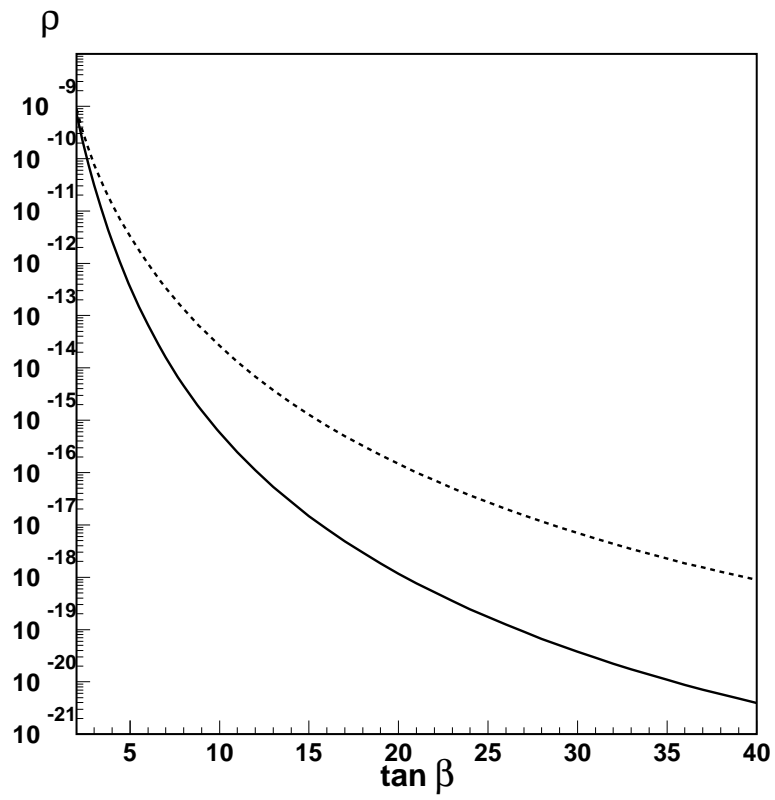


Fig. 3: The plot of ρ , as a function of $\tan \beta$ for $\mu_1 = 5$ (solid curve) and $\mu_1 = 3.5$ (dashed curve). The remaining parameters are the same as Fig. 1.

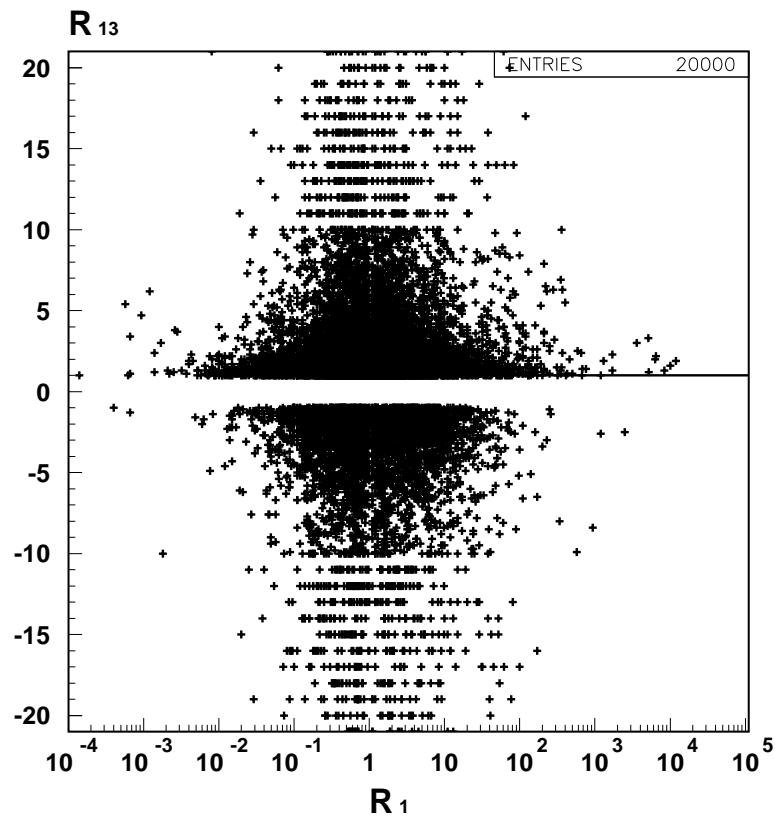


Fig. 4a: The plot of R_{13} against R_1 , under the condition of $(m_{h_{(n+1)}} - m_{h_{(n)}}) > 10 \text{ GeV}$, where $n = 1$ to 4.

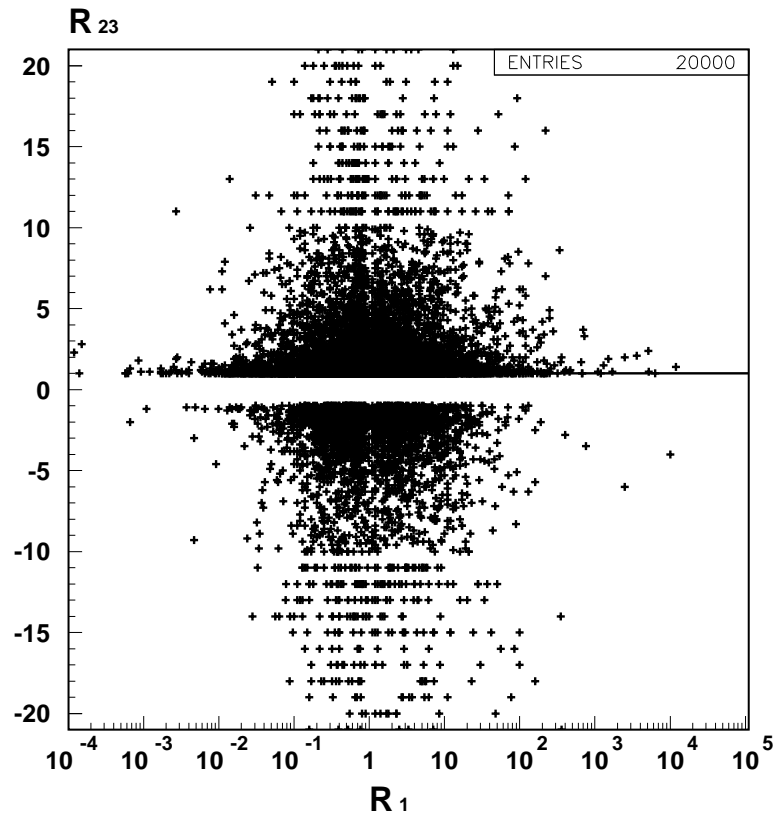


Fig. 4b: The plot of R_{23} against R_1 , under the condition of $(m_{h_{(n+1)}} - m_{h_{(n)}}) > 10 \text{ GeV}$, where $n = 1$ to 4.

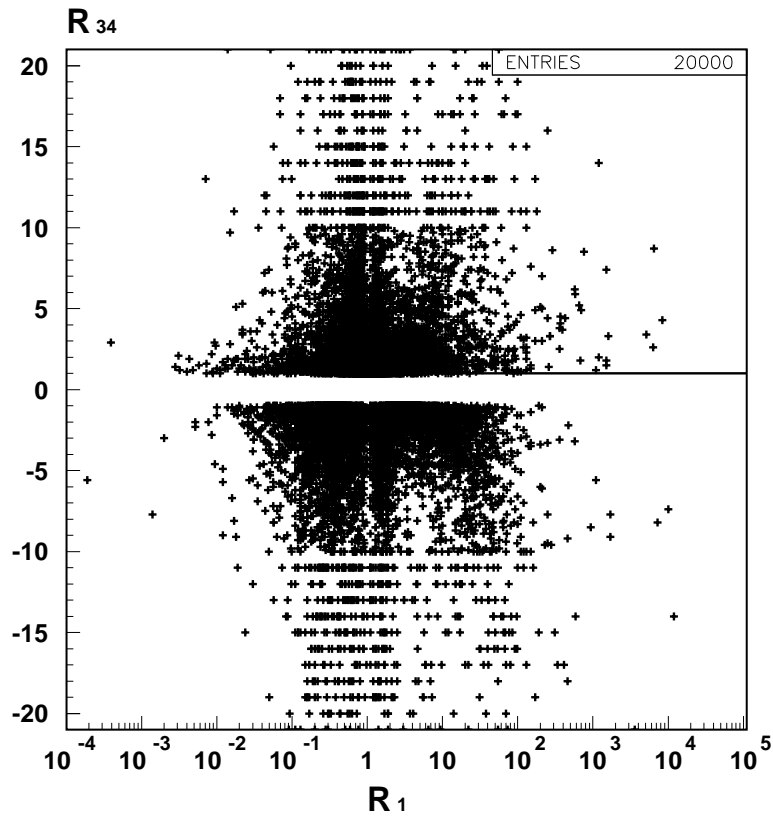


Fig. 4c: The plot of R_{34} against R_1 , under the condition of $(m_{h_{(n+1)}} - m_{h_{(n)}}) > 10 \text{ GeV}$, where $n = 1$ to 4.

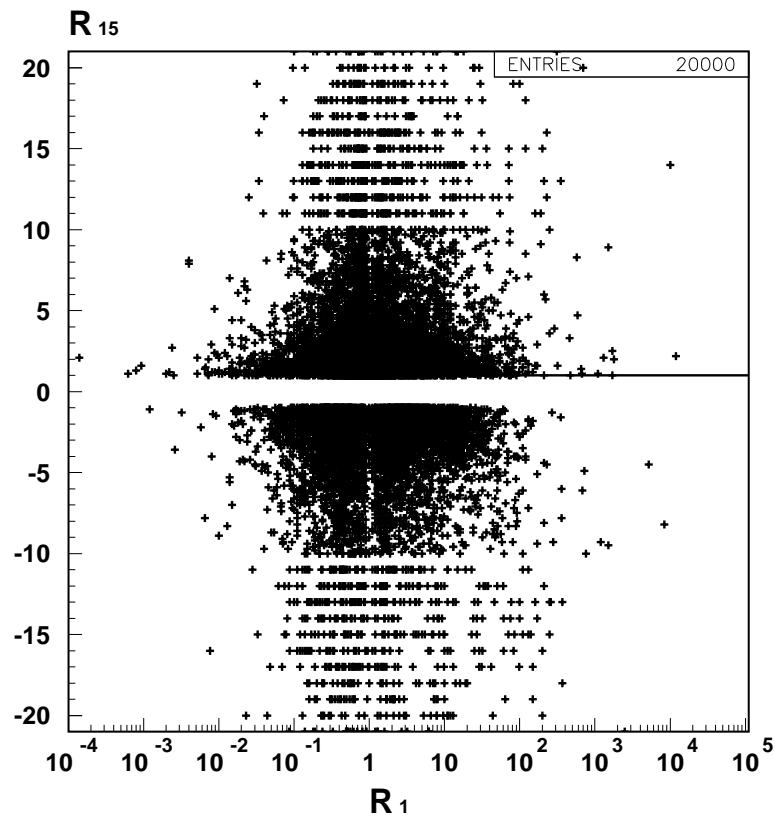


Fig. 4d: The plot of R_{15} against R_1 , under the condition of $(m_{h_{(n+1)}} - m_{h_{(n)}}) > 10 \text{ GeV}$, where $n = 1$ to 4.

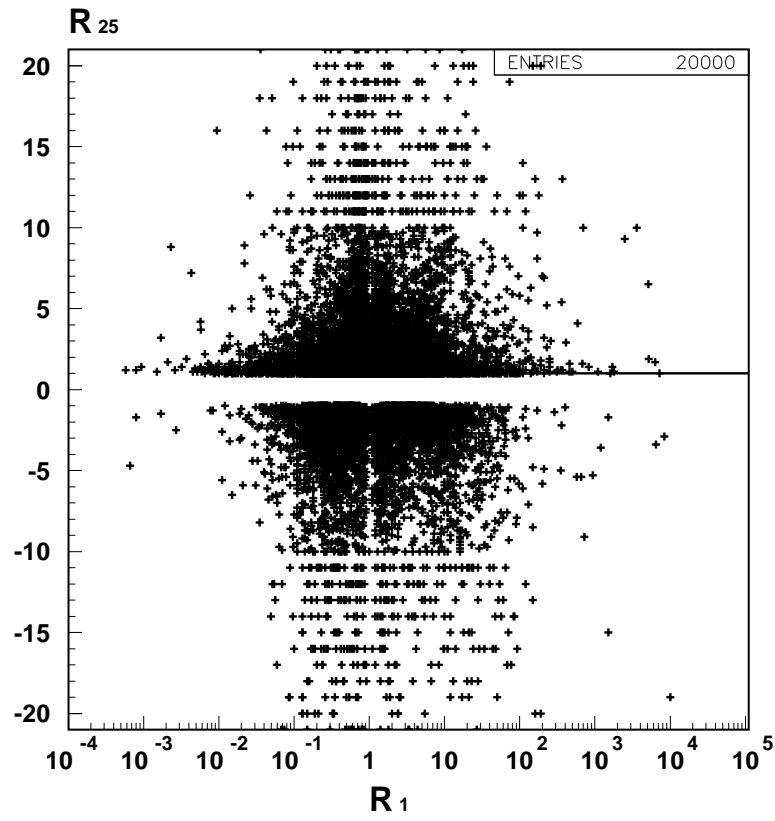


Fig. 4e: The plot of R_{25} against R_1 , under the condition of $(m_{h_{(n+1)}} - m_{h_{(n)}}) > 10 \text{ GeV}$, where $n = 1$ to 4.

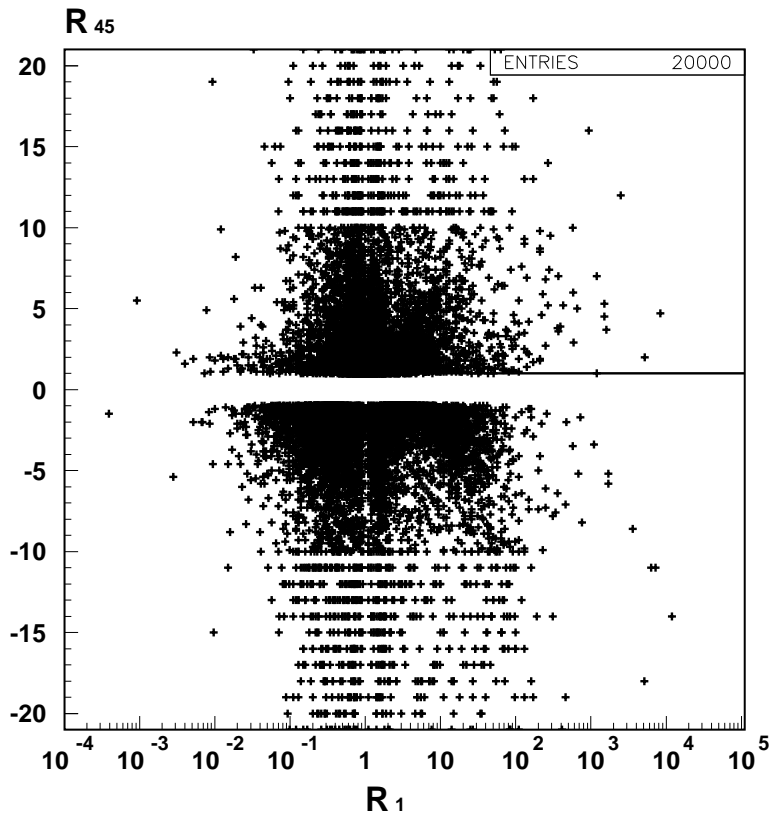


Fig. 4f: The plot of R_{45} against R_1 , under the condition of $(m_{h_{(n+1)}} - m_{h_{(n)}}) > 10 \text{ GeV}$, where $n = 1$ to 4.

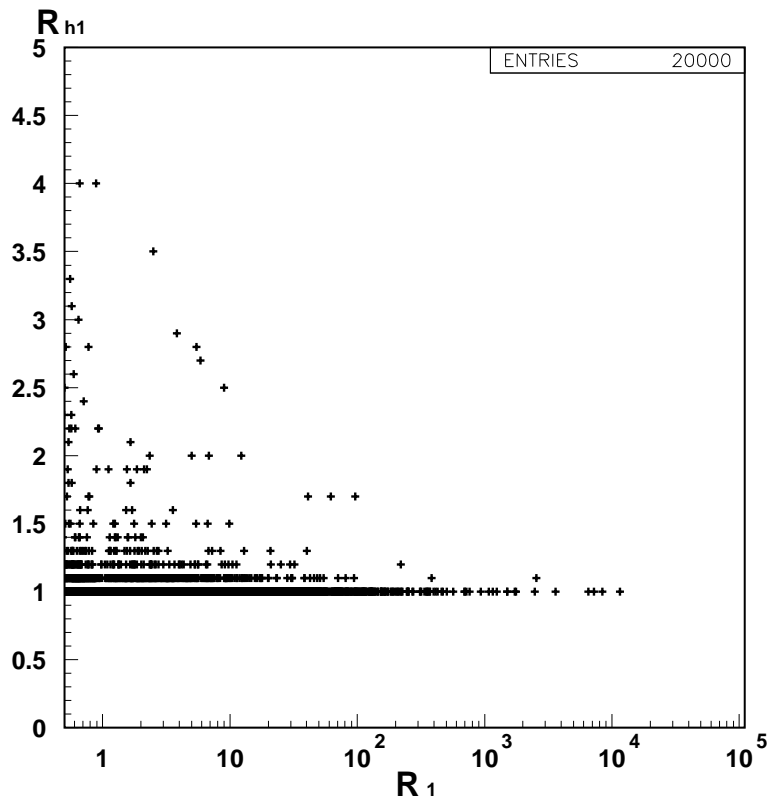


Fig. 5: The plot of R_{h1} against R_1 , under the condition of $(m_{h_{(n+1)}} - m_{h_{(n)}}) > 10 \text{ GeV}$, where $n = 1$ to 4.